(12) INTERNATIONAL APPLICATION PUBLISHED UNDER THE PATENT COOPERATION TREATY (PCT)

(19) World Intellectual Property Organization
International Bureau

(43) International Publication Date
13 June 2002 (13.06.2002)

PCT

(10) International Publication Number
WO 02/47223 A1

(51) International Patent Classification[7]: H01S 5/183, 5/04

(21) International Application Number: PCT/GB01/05387

(22) International Filing Date: 5 December 2001 (05.12.2001)

(25) Filing Language: English

(26) Publication Language: English

(30) Priority Data:
0030015.2 8 December 2000 (08.12.2000) GB

(71) Applicant *(for all designated States except US)*: **UNIVERSITY OF SOUTHAMPTON** [GB/GB]; Highfield, Southampton SO17 1BJ (GB).

(72) Inventor; and

(75) Inventor/Applicant *(for US only)*: **GARNACHE-CREUILLOT, Arnaud** [GB/GB]; c/o Centre for Enterprise & Innovation, University of Southampton, Highfield, Southampton SO17 1BJ (GB).

(74) Agents: **HAINES, Miles, John** et al.; D Young & Co, 21 New Fetter Lane, London EC1A 1DA (GB).

(81) Designated States *(national)*: AE, AG, AL, AM, AT, AU, AZ, BA, BB, BG, BR, BY, BZ, CA, CH, CN, CO, CR, CU, CZ, DE, DK, DM, DZ, EC, EE, ES, FI, GB, GD, GE, GH, GM, HR, HU, ID, IL, IN, IS, JP, KE, KG, KP, KR, KZ, LC, LK, LR, LS, LT, LU, LV, MA, MD, MG, MK, MN, MW, MX, MZ, NO, NZ, OM, PH, PL, PT, RO, RU, SD, SE, SG, SI, SK, SL, TJ, TM, TR, TT, TZ, UA, UG, US, UZ, VN, YU, ZA, ZM, ZW.

(84) Designated States *(regional)*: ARIPO patent (GH, GM, KE, LS, MW, MZ, SD, SL, SZ, TZ, UG, ZM, ZW), Eurasian patent (AM, AZ, BY, KG, KZ, MD, RU, TJ, TM), European patent (AT, BE, CH, CY, DE, DK, ES, FI, FR, GB, GR, IE, IT, LU, MC, NL, PT, SE, TR), OAPI patent (BF, BJ, CF, CG, CI, CM, GA, GN, GQ, GW, ML, MR, NE, SN, TD, TG).

Published:
— *with international search report*

[Continued on next page]

(54) Title: OPTICALLY PUMPED VERTICAL CAVITY SEMICONDUCTOR LASER DEVICE

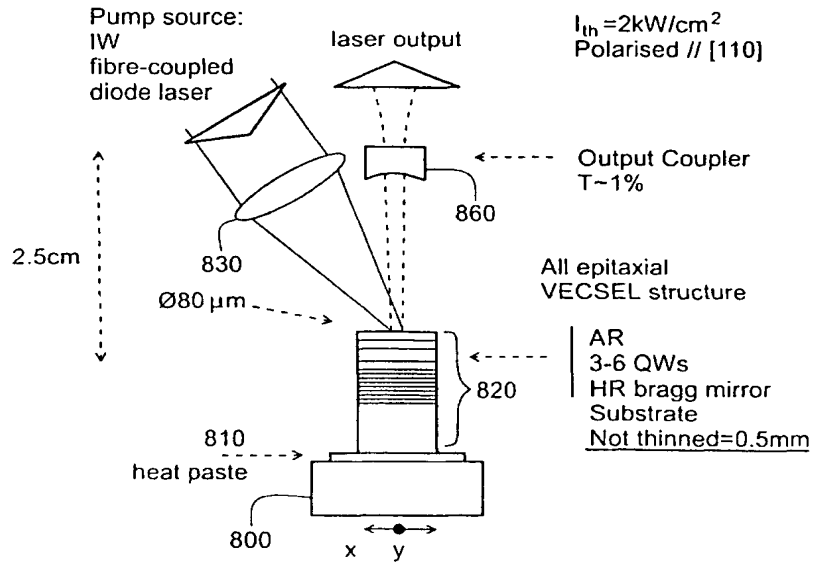

(57) Abstract: A vertical cavity laser device comprises a multi-layer laser structure (820) having a pump light receiving face (90, 70) for receiving incident pump light at a pump wavelength, and a semiconductor gain region (30B) operable to provide optical gain at a laser emission wavelength in response to the pump light; two laser cavity mirrors disposed about the multi-layer laser structure so as to define a laser cavity wherein each laser cavity mirror is operable to reflect light at the laser emission wavelength; and a pump mirror (60, 80) disposed behind the gain region (30B) so as to reflect pump light back through the gain region (30B) for at least a second pass.

WO 02/47223 A1

For two-letter codes and other abbreviations, refer to the "Guidance Notes on Codes and Abbreviations" appearing at the beginning of each regular issue of the PCT Gazette.

OPTICALLY PUMPED VERTICAL CAVITY SENICONDUCTOR LASER DEVICE

The invention relates generally to semiconductor lasers and in particular to vertical external cavity surface-emitting semiconductor lasers.

Compact lasers with output powers of at least Watt-level with good spatial beam profiles have applications including optical communications, high-density optical storage, laser radar, materials processing and laser absorption spectroscopy. High optical power and diffraction-limited circular laser-beam profiles enable beam propagation over large distances and focusing of high power into small areas.

It is difficult to produce a semiconductor laser output beam that is high-power, circular and diffraction limited. Conventional semiconductor lasers can emit single-transverse-mode beams but only at powers considerably less than 1 Watt . Higher power (1-11 W) output is achievable using semiconductor lasers known as "wide-stripe" lasers. Wide-stripe lasers typically have output that is multi-transverse mode but where single-transverse mode output is possible, elaborate optics is required for reshaping of the strongly astigmatic beam which is produced.

The vertical-cavity surface-emitting laser (VCSEL) is a known type of electrically pumped semiconductor micro-cavity laser that offers the advantages of high-speed, dynamic, single-longitudinal-mode operation; output in a circular astigmatism-free beam; and good electrical to optical power conversion efficiency. The VCSEL micro-cavity is formed from a multiple quantum well (QW) active region placed between multi-layer "Bragg stack" mirrors disposed at the front and the back of a semiconductor chip. The VCSEL devices require a highly reflecting back mirror and a front mirror of lower reflectivity. In practical terms the VCSEL is limited because it has low output power and cannot deliver more than about 3mW in a diffraction-limited beam. The diffraction limited beam is typically achieved using small (~ 6μm) diameter VCSEL devices resulting in a disadvantageously large beam divergence (6° half-angle). A further disadvantage of the VCSEL is that the line-width of the laser output is ~10 MHz which is broader than is desirable for practical applications.

The disadvantages of the VCSEL have been partially overcome by increasing the size of the laser cavity which is achieved by replacing the front multi-layer Bragg

mirror by an external concave mirror. This results in a structure known as a vertical-external-cavity surface-emitting laser (VECSEL). The lasing cavity of the VECSEL is formed between the high reflectivity Bragg mirror on the semiconductor chip at the back end and the external concave mirror at the front. The cavity length is typically in the range from μm (10^{-6}m) to cm (10^{-2}m). The external cavity enables production of a diffraction-limited beam output at high (Watt-level) power; reduces the laser line-width in single mode operation; and allows the incorporation of intra-cavity elements. The replacement of the front Bragg stack mirror by an external concave mirror allows the VECSEL to be designed to operate at wavelengths where the reflectivity of the Bragg stack mirrors is low, for example, at around 1.5 μm.

VECSELs can be optically pumped rather than electrically pumped to create optically pumped semiconductor (OPS) VECSELs which combine the advantageous features of diode-pumped solid state lasers and VCSELS. OPS VECSELs typically use a commercial multimode laser diode pump which is focussed onto the semiconductor chip. The diode pump generates optical power, a group of QWs provide gain and the external mirror controls the output modes of the laser. The use of optical pumping means that a large optical mode area can be used for high power operation which reduces susceptibility to optical damage and gives low beam divergence. Since optically pumped laser devices can be made electrically insulating they are less likely optically lossy and are simpler to fabricate. In comparison with other diode-pumped solid-state lasers OPS VECSELS offer the advantage that the laser medium has a broad (>40nm) pump bandwidth. This ensures efficient absorption of the spectrally broad pump-diode light, eliminates sensitivity to pump-diode and wavelength variation and also eliminates the requirement for pump-diode lasers with tight wavelength specifications. The main requirement for OPS VECSELS is that the pump wavelength should be greater than the bandgap energy of the active region.

Figure 1 is a schematic diagram of a typical OPS-VECSEL. A laser diode pump 10 emits light 15 at a pump wavelength λ_P. The light emanating from the laser diode 10 is passed through a lens 20 which focuses a light beam 25 into an "active region" 30B of a VECSEL structure known as a gain mirror 30. The gain mirror 30

has three main layers comprising a multi-layer mirror 30C, the active region 30B and an anti-reflection coating 30A.

The multi-layer mirror 30C is a highly reflective Bragg stack. Bragg stacks are composed of layer-pairs, each pair having a layer of high and a layer of low refractive index material. A number of layer-pairs are placed between two homogeneous media which in this case are the substrate and air. The reflectivity R of the Bragg stack is dependent on the refractive index difference between the materials and the number of pairs of alternate layers used. The reflectivity is expressed by the formula:

$$R = \left(\frac{1 - \frac{n_s}{n_0}\left(\frac{n_1}{n_2}\right)^{2N}}{1 + \frac{n_s}{n_0}\left(\frac{n_1}{n_2}\right)^{2N}} \right)^2$$

where n_1 and n_2 are the refractive indices of the materials forming each layer-pair, n_s and n_0 are the refractive indices of the substrate and incident medium respectively; and N is the number of periods of layer-pairs. This formula shows that if N is fixed, the reflectivity increases when the ratio n_1/n_2 is increased and conversely if n_1/n_2 is fixed, the reflectivity increases with N. Many Bragg stacks use quarter-wave films for which the optical thickness of each layer is $\lambda_0/4$ where λ_0 is the wavelength *in vacuo*. If the thickness of the layer with refractive index n_1 is h_1 and the thickness of the layer with refractive index n_2 is h_2 then the dimensions of the quarter-wave stack are chosen such that $n_1h_1=n_2h_2=\lambda_0/4$.

The Bragg stack mirror 30C could for example be constructed from pairs of AlAs/GaAs quarter-wave layers. Since this mirror forms the back mirror of the lasing cavity it is designed to be highly reflective at the laser output wavelength λ_L. Thus the layers are constructed with an optical thickness of $\lambda_L/4$.

The active region 30B comprises a multiplicity of quantum wells, which are typically formed by sandwiching one thin low-band-gap material between two higher-band-gap materials. Typically electrons are trapped in the region with the lower

band-gap but they have a finite probability of tunnelling through the high-band-gap barriers. The active region absorbs the incoming light 25 from the optical pump. Electrons and holes, which are "carriers", are generated in the active region by the light from the optical pump. These photo-excited carriers diffuse through the active region and are captured by the multiple QWs that provide gain across a predetermined range of wavelengths. The gain is typically inversely proportional to the thickness of the active region.

A standing wave is set up in the chip micro-cavity and the length of the active region is arranged so that the maxima of the intra-cavity standing wave coincide with the locations of the QWs. The electrons and holes are confined to the active region by an anti-reflection (AR) coating 30A which separates the active region 30B from an air interface in the main laser cavity. The AR coating 30A is designed to have low reflectivity and thus improved transmissivity at λ_L which increases the intensity of laser light entering the main laser cavity 45.

The AR coating 30A typically has a broadband absorption profile to improve pump light transmission into the semiconductor. This AR coating is formed from a layer of a dielectric material and a confinement layer that is needed to prevent carriers from diffusing to the semiconductor surface. Since the materials of the AR layer 30A have a high energy gap, the pump radiation at λ_p is not absorbed inside this layer. The main laser cavity 45 is bounded by an external concave mirror 50 at the front and by the highly reflective Bragg micro-mirror 30C at the back. The laser can be tuned by adjusting the length of the laser cavity 45. The laser can also be tuned by altering the position of the incident pump light on the gain mirror structure. By exploiting non-uniformities in the gain mirror structure a shift in the reflection wavelength of the Bragg mirror 30C can thus be achieved. The wavelength of the output laser light 55 is determined both by the particular modes of vibration supported in the cavity, which depend on the length of the laser cavity 45, and by the peak wavelength of the effective gain.

The gain mirror 30 forms a micro-cavity that must be coupled to the main laser cavity 45. To maximise the tuning range of the laser it is important that this coupling is as wavelength-insensitive as possible. A wavelength-insensitive coupling

also reduces the interplay between optical and thermal effects. Since optical properties such as refractive indices are very sensitive to temperature changes, poor coupling between the micro-cavity and the main laser cavity 45 is disadvantageous as it may result in the output power of the laser device attaining a maximum at a small value of the incident pump power. Thereafter, further increasing the pump power will cause a rapid decrease in the output power of the device which may then switch-off due to "thermal rollover".

The gain mirror 30 is attached to a heat-sink 40. The heat-sink may be mounted on a thermoelectric cooler, in which case, fine wavelength tuning can be achieved by changing the gain mirror temperature.

A first prior art design for the gain mirror 30 aims to improve pump power absorption in the gain mirror 30 by making the active layer relatively wide (several μm) and incorporating within it a large number of QWs. The micro-cavity of the gain mirror is typically designed to operate at resonance. The electric field amplitude of the mode in the active region is a maximum at the location of the QWs. This gain mirror design does increase the absorbed laser pump power but has the disadvantage of increased temperature sensitivity as a direct result of its narrow spectral window of operation.

A second prior art design for the gain mirror 30 is described in the research paper "Diode-pumped broadband Vertical-External-Cavity surface Emitting semiconductor laser: Application to high sensitivity intracavity laser absorption spectroscopy", A. Garnache et al., JOSA B, September 2000[1]. This design increases the spectral bandwidth of the coupling between the active region 30B and the main laser cavity 45 by using an AR coating 30A that is narrow-band and by designing the micro-cavity of the gain mirror so that it operates at anti-resonance. It has used an active region which is thinner than for the first prior art design.

The narrow-band AR coating is essentially a Bragg stack comprising a multiplicity of dielectric layers. The reflection at the gain mirror interface with the air (i.e. at the interface of AR coating 30A with the air in the laser cavity) is significantly larger than the reflection at the interface between the layers in the active zone. Thus the space between the surface of the AR coating at the air interface and

the highly reflective Bragg stack 30C at the opposite end of the gain mirror acts as a sub-cavity. The sub-cavity works at anti-resonance at the design wavelength λ_L, hence the sub-cavity length is not a multiple of $\lambda_L/4$. However the narrow-band response of the AR stack 30A results in a resonance condition being set up at some other wavelength λ_R, where the sub-cavity length is a multiple of $\lambda_R/2$. Since the effective gain is proportional to the product of the material gain produced by the QWs in the active region and the modulus squared of the electric field $|E|^2$, the net effect of the AR stack is to increase the effective gain bandwidth of the gain mirror 30. The AR-stack bandwidth is designed to approximately match the free spectral range (FSR) between the two sub-cavity modes i.e. the mode associated with $\lambda_L/4$ and the mode associated with $\lambda_R/2$. As a result the gain mirror has a filter profile with a shape like a top-hat and it is considerably broader than the single-peak curve characteristic of the intrinsic gain bandwidth.

In the case of the first prior art design where the AR coating 30A is a single half-wave layer, rather than a multi-layer stack, the resonance at λ_R is absent because the region between the highly reflective Bragg mirror 30C and the surface of the AR coating 30A at the air interface looks like a single optical layer. In this case reflections at the air interface will be present at any wavelength and not restricted to a narrow band. The absence of the resonance due to reflection at the air interface means that the effective gain bandwidth will be narrower for the first prior art design than for the second prior art design.

The second prior art design for the gain mirror 30 has the advantage that it increases the gain bandwidth and hence improves the coupling between the microcavity and the main laser cavity in the region of the spectrum close to the laser wavelength λ_L. However, this design has the disadvantage that the incoming laser diode pump energy is inefficiently converted into laser output. The multilayer structure of the AR coating is specially designed to provide good coupling between the microcavity and the main laser cavity at wavelengths close to the laser wavelength λ_L. As a consequence, the AR coating is more reflective (typically 30% or greater) at the pump wavelength λ_P than it would be in the case of the first prior art design.

The fact that the active region of the second prior art design is narrow has the disadvantage that a relatively small proportion of the laser diode pump light entering the active region is absorbed there. The wasted fraction of light (around 50%) is dissipated as heat which can cause a decrease in the output power due to thermal rollover.

The invention provides a vertical cavity laser device comprising:

a multi-layer laser structure having a pump light receiving face for receiving incident pump light at a pump wavelength, and a semiconductor gain region operable to provide optical gain at a laser emission wavelength in response to the pump light;

two laser cavity mirrors disposed about the multi-layer laser structure so as to define a laser cavity wherein each laser cavity mirror is operable to reflect light at the laser emission wavelength; and

a pump mirror disposed behind the gain region so as to reflect pump light back through the gain region for at least a second pass.

Embodiments of the invention provide a gain with a broad spectral bandwidth that improves the coupling of the micro-cavity to the main laser cavity at the laser wavelength and, in addition, they provide improved efficiency of conversion of pump laser light to laser output. Thus embodiments of the invention offer the advantageous features of both the first and second prior-art designs discussed above.

The gain region can preferably be a multi-layered structure, for example a quantum well structure as in previously proposed VECSELs.

Further respective aspects and features of the invention are defined in the appended claims.

Embodiments of the invention will now be described by way of example only with reference to the accompanying drawings, in which:

Figure 1 is a schematic diagram of an OPS VECSEL;

Figure 2A is a schematic diagram of a gain mirror structure according to a first embodiment of the invention;

Figure 2B is a schematic diagram of a gain mirror structure according to a second embodiment of the invention;

Figure 3 is a band-energy diagram for a DP VECSEL according to a first embodiment of the invention;

Figure 4 is a table that specifies the design parameters of the DP VECSEL of the first embodiment of the invention;

Figure 5 is the mathematically predicted behaviour of the anti-reflection coating according to the first embodiment of the invention;

Figure 6 shows the predicted behaviour of reflectivity and the modulus squared of the electric field in the quantum wells as a function of wavelength for the first embodiment of the invention;

Figure 7 shows the predicted behaviour of the Bragg reflectivity of the highly reflective mirror of the first embodiment of the invention;

Figure 8 shows the predicted value modulus squared of the electric field across the whole DP VECSEL structure according to the first embodiment of the invention;

Figure 9 shows an experimental set-up suitable for both the first embodiment and the second embodiment of the invention;

Figure 10 shows experimental results for reflectivity as a function of wavelength for the whole gain-mirror structure according to the first embodiment of the invention;

Figure 11 shows experimental results for reflectivity as a function of wavelength for the anti-reflection coating according to the first embodiment of the invention;

Figure 12 shows experimental results for the reflectivity and the photoluminescence as functions of wavelength for the epitaxial VECSEL structure according to the first embodiment of the invention;

Figure 13 shows experimental results for output power as a function of input power according to the first embodiment of the invention;

Figure 14 shows experimental results for differential quantum efficiency and wavelength functions of incident pump power according to the first embodiment of the invention;

Figure 15 is a band gap energy diagram for a CEP VECSEL according to a second embodiment of the invention;

Figure 16 is a table that specifies the parameters of the CEP VECSEL of the second embodiment of the invention;

Figure 17 is the mathematically predicted behaviour of the highly reflective Bragg mirror according to the second embodiment of the invention;

Figure 18 shows the predicted behaviour of the anti-reflection coating of the second embodiment of the invention;

Figure 19 shows the predicted reflectivity and transmissivity in the whole structure as a function of wavelength according to the second embodiment of the invention;

Figure 20 shows the predicted behaviour of reflectivity and the modulus squared of the electric field in the active region in the region of the laser emission wavelength for the second embodiment of the invention; and

Figure 21 shows the predicted behaviour of reflectivity and the modulus squared of the electric field in the active region in the region of the pump wavelength for the second embodiment of the invention.

Figure 2 illustrates schematically two alternative constructions for the gain mirror according to embodiments of the invention. Figure 2A illustrates a "double pass pumping" gain mirror structure 100. This modifies in two ways the gain mirror of the second prior-art design. The basic components as already described above are the multi-layer anti-reflection coating 30A which has high transmittance at the laser wavelength, the active region 30B including QWs, and the Bragg stack mirror 30C which is highly reflective (HR) at the laser wavelength. The first modification is the addition of an AR multi-layer structure that has high transmissivity and low reflectivity at the pump wavelength. This modification results in a dual-wavelength AR structure that is anti-reflecting at both the laser wavelength and at the pump wavelength. The reflectivity of this dual-wavelength AR structure comprising layers 30A and 70 is typically less than 5% over a wavelength range that is broad enough to accept wavelength instability of the pump laser and to accommodate a possible wavelength shift due to heating of the gain mirror. This first modification serves to reduce reflection loss of the pump light at the air interface.

The second modification included in the double pump pass pumping gain mirror is the addition of a further Bragg stack mirror 60 that is highly reflective at the pump wavelength. This additional mirror 60 is located behind the mirror 30C and serves to reflect pump light that has made a single pass through the active region,

directing it back for a second pass through the micro-cavity. This modification serves to double the effective absorption path that the active region presents to the pump laser light. The two highly reflective mirrors 60 and 30C are substantially non-absorbent to either the pump or the laser light because these mirrors have large energy band-gaps. This gain mirror structure will promote a more uniform distribution of electron and hole carriers amongst the QWs in the active region 30B. Note that this structure allows optical pumping from a single direction only such that the pump light is incident on the side of the gain mirror with the AR coating.

A "cavity-enhanced pumping" gain mirror structure 200 is shown in Figure 2B. In this case the gain mirror of the second prior-art design comprising a mirror 30C highly reflective at λ_L, a thin active region 30B and an anti-reflection stack 30A with high transmissivity at λ_L is modified by adding a first additional mirror 80 and a second additional mirror 90, with one on either side of three-layer gain mirror structure (30A, 30B, 30C). In this embodiment of the invention the reflectivity of the first additional mirrors 80 is close to 100% and the reflectivity of additional mirror 90 is around 30%. The reflectivity of the first additional mirror 80 could be in the range from 50% to 100% while the reflectivity of the second additional mirror 90 could be in the range from 10% to 60%. These two additional mirrors 80 and 90 define an optical cavity inside the multi-layer structure that is designed to operate resonantly at the pump wavelength. The outer cavity is designed so that the separation in wavelength between the resonant peaks is small. The cavity has low finesse and the resonance, which is centred on the pump wavelength, is spectrally broad. This cavity enhanced pumping structure for the gain mirror reduces the reflectivity at the pump wavelength and the cavity formed by the additional mirrors 80 and 90 promotes multiple passes of the pump light through the active region. The design equation that gives a relationship between the reflectivities of the first and second additional mirrors 80 and 90 is:

$$R2_{\lambda p} = R1_{\lambda p} e^{-\alpha_{\lambda p} w}$$

where $R1_{\lambda p}$ is the reflectivity of the first additional mirror 80; $R2_{\lambda p}$ is the reflectivity of the second additional mirror 90; $\alpha_{\lambda p}$ is the absorption coefficient at λ_p; and w is the thickness of the absorber in the active region.

The active region of the cavity enhanced gain mirror can be made thinner than the active region for the double-pass pumping structure 100. Both of the gain mirrors illustrated in Figure 2 should allow the OPS-VECSEL to be pumped optically with efficiency greater than $0.9\times(\lambda_P/\lambda_L)$. This can be achieved without increasing the length of the active region. The quantum efficiency can be improved by keeping the optical pump photon energy close to the laser photon energy. The improved efficiency reduces heating of the gain mirror.

The multi-layer structure of the anti-reflection coating and the high and medium reflectivity Bragg stack mirrors can be grown in a single fabrication process known as "epitaxy" where the layers are grown on top of each other such that the crystal orientation of the upper layer is determined by the crystal orientation of the base layer. Alternatively the multi-layer structures can be fabricated as composites formed by depositing additional layers on epitaxially grown structures. The structures are designed for their optical properties alone and they are electrically insulating. In the embodiments of the invention described below the multi-layered structures of the Bragg mirrors and of the anti-reflection coatings are generally periodic structures comprising layers of optical thickness $\lambda/4$. Such layered structures are suitable for the growth of GaAs. However the multi-layered structures could also be non-periodic structures comprising dielectric layers with differing thicknesses. Any multi-layered structure with the reflectivity in the region of λ_L and λ_P properties in accordance with the invention would suffice.

Figure 3 is a band-gap energy diagram for an embodiment of the double pass pumping structure 100 (DP VECSEL). In this embodiment λ_L=1020nm and λ_P=820nm. The optical pump light 505 enters the gain mirror through the composite AR layer 535 and passes through the active region 30B where a proportion of the pump energy is absorbed. The pump light that is not absorbed in the active layer will pass through the HR layer 525 designed to reflect at λ_L and will be reflected by the distributed Bragg reflector (DBR) 545 such that it passes back through the active region for a second time. The light 515 at λ_L=1020nm generated by the active region is reflected from the HR mirror 525 and passes through the AR structure into the main laser cavity 600. The gain mirror is formed on a gallium arsenide (GaAs)

substrate 590 whose band-energy is smaller than that of the pump laser but larger than that of the main laser. The active region 30B comprises six QWs 500 formed from very thin layers of indium gallium arsenide (InGaAs). The QWs 500 are arranged in a (2+1+1+2) formation and are separated by layers of GaAs. The optical depth of the active region is 5.1 times $\lambda_L/2$. This value of 5.1 takes account of the phase-shift of the laser light due to reflection at the multi-layer AR stack 535. The structure is designed to be anti-resonant at the laser wavelength, which means that there is a node at the air/semiconductor interface. The quantum wells are placed at the anti-nodes of the intra-cavity standing wave 570 as shown.

The Bragg stack 545 which has high reflectivity at λ_P comprises eight pairs of layers 510. Each pair 510 consists of an $Al_{0.1}Ga_{0.9}As$ layer of optical thickness $\lambda_P/4$ and an AlAs layer of optical thickness $\lambda_P/4$. The band-energy of AlAs is higher than that of the $Al_{0.1}Ga_{0.9}As$ so a series of potential wells is formed.

The HR mirror 525 adjacent to the HR mirror 545 comprises twenty-seven pairs 520, each of which comprises a layer of AlAs and a layer of AlGaAs. Each layer has an optical thickness of $\lambda_L/4$. A single additional $\lambda_L/4$ layer 521 of AlAs is situated adjacent to these twenty-seven pairs and to the active region. The anti-reflection coating 535 comprises a multi-layer structure with the layer spacing as specified in Figure 4, arranged to give an optical depth of $\lambda''/4$ with $\lambda'' = 903$nm. The value λ'' is the appropriate value so that the multi-layer structure has low reflectivity at both of the wavelengths λ_L and λ_P. The design equation that gives the appropriate wavelength λ_{DW} that specifies the optical depths of a multi-layer structure which provides high reflectivity in dual wavelength (DW) bands centred on λ_L and λ_P is:

$$\lambda_{DW} = \frac{2\lambda_P\lambda_L}{(\lambda_P + \lambda_L)}$$

This design equation gives λ_{DW} =909nm for λ_L =1020 and λ_P=820 but does not take account of dispersion. The quoted value of $\lambda'' = 903$nm has been adjusted from λ_{DW} to account for dispersion effects.

The AR coating 535 consists of a unit 530 comprising a pair of $\lambda''/4$ layers of AlAs and AlGaAs which is repeated twice, a single $\lambda''/4$ layer 531 of AlAs, a $\lambda''/2$

layer 540 of AlGaAs and an AlAs/AlGaAs/AlAs triplet 550 of $\lambda''/4$ layers. There is a "caping layer" 580 of GaAs approximately 8nm wide at the air interface and the layer of AlAs adjacent to this caping layer has an optical thickness of slightly less than $\lambda''/4$ thick to accommodate the caping layer.

Figure 4 is a table that specifies the composition of each of the multi-layer structures corresponding to the band gap diagram of Figure 3 and specifies the spacings or material thickness of each layer required to obtain the appropriate optical thickness. The optical thickness is given by the product of the layer spacing and the refractive index of the respective layer. The refractive indices at 1050nm are given by Table 1 below.

Material	**Refractive index at 1050nm**
AlAs	2.94
GaAs	3.49
$Al_{0.12}Ga_{0.88}As$	3.435
$Al_{0.15}Ga_{0.85}As$	3.42
$Al_{0.05}Ga_{0.95}As$	3.47

Figures 5 to 8 are predictions obtained from mathematical models of the DP VECSEL structure of Figure 3.

Figure 5 is a plot of reflectivity against wavelength for the composite AR layer 535 of the embodiment of the DP VECSEL corresponding to Figure 3. In this case the reflectivity is substantially zero at λ_L =1020 and at λ_P=820. The trough in reflectivity at around λ_L =1020 is narrower than it would typically be for prior art anti-reflection coatings.

Figure 6 is a plot of the square of the absolute value of the electric field E in the QWs 500 of the active region of the DP VECSEL. The dashed double-peak curve 710 corresponds to a QW on the side of the anti-reflection coating 535 while the solid double-peaked curve 700 corresponds to a QW on the side of the high reflectivity Bragg stack mirror 525. The uppermost solid line 720 is a plot of reflectivity against

wavelength for the whole gain mirror structure which has a top-hat shape with a constant value over a broad range of wavelengths centred around 1020 μm.

Figure 7 shows the Bragg reflectivity for the DP VECSEL, which is the squared coefficient of reflectivity for the electric field, as a function of wavelength. The plot is for the pump DBR 545 and the HR mirror 525 part of the gain mirror structure only. The Bragg reflectivity is high with a value greater than 0.8 at λ_P=0.82μm=820nm and reaches a maximum value of 1.0 over a wavelength range from 0.98 μm to 1.06 μm. The broad maximum encompasses the laser emission wavelength λ_L=1.02μm=1020nm.

Figure 8 shows the spatial distribution of the square of the absolute value of the electric field $|E|^2$ in the gain mirror structure at the laser emission wavelength λ_L for the DP VECSEL. Since the AR coating has negligible reflectivity at its design wavelength, the energy flux in the air and in the active zone is approximately the same for both the incident and for the reflected wave. As a consequence $|E|^2$ in the active region is lower than that in air by a factor equal to the refractive index of GaAs.

Figure 9 shows an experimental set-up for implementing the double-pass pumping OPS-VECSEL according to a first embodiment of the invention. The gain mirror structure is mounted on a copper heat-sink 800 using a layer of heat paste 810. The gain mirror structure 820 comprises from bottom to top: the GaAs substrate; the highly reflective Bragg stack mirror; the active region containing from three to six QWs; and the anti-reflection coating. The VECSEL gain mirror structure is fabricated epitaxially. The optical pump source 870 is located about 2.5cm from the active region of the gain mirror. The pump light is incident on the gain mirror at a slight angle and it is focused by a convex lens 830.

The external concave mirror 860 of the main laser cavity which acts as an output coupler has a transmissivity of around 1% at the laser wavelength and is located directly above the gain mirror, at a distance of about 2.5cm from the top of the active zone. The laser output is directed through the concave mirror 860.

Figures 10 to 14 are experimental results obtained using the set-up of Figure 9.

Figure 10 gives the reflectivity as a function of wavelength for seven different values of the displacement d in mm of the incident laser pump light from the centre of

the gain mirror structure for the whole VECSEL structure including the Bragg HRs 545and 525, the active region 505 and the AR region 535. Curve 900 corresponds to zero displacement of the pump light incident from the centre of the gain mirror and curve 960 corresponds to a displacement of 17.5mm from the centre. This figure illustrates that if the gain mirror multi-layer structure is designed for λ_L and λ_P at zero displacement, the gain mirror characteristics are effectively blue-shifted to smaller wavelengths by increasing the displacement d. This is the reason why the design wavelength used for the second embodiment of the invention illustrated in Figures 15 and 16 is 1050nm rather than 1020nm.

Figure 11 gives the reflectivity as a function of wavelength for the anti-reflection coating 535 of the first embodiment of the invention. These results are in good agreement with the prediction of the mathematical model shown in Figure 5.

Figure 12 characterises the DP VECSEL structure according to the first embodiment of the invention. The uppermost curve 1020 gives the reflectivity of the gain mirror as a function of wavelength. The middle curve 1010 gives the edge photoluminescence of the gain mirror as a function of wavelength, which was obtained by pumping close to the edge of the wafer. The lowermost curve 1000 gives the surface photoluminescence of the gain mirror as a function of wavelength. In this case λ_L=1020nm and the incident laser pump power was 100mW.

Figure 13 gives the output power P_{out} in mW as a function of P_{in} on the chip in Watts. The output power rises approximately linearly from zero at P_{in} =0.1W to a maximum value of around 400mW at P_{in} ~ 1.3W. This figure illustrates the damage ratio of the gain mirror structure due to high intensity at λ_L inside the cavity.

Figure 14 gives two parameters as a function of the incident pump power P_{in} on the chip in Watts. The uppermost curve 1050 is the differential quantum efficiency dP_{out}/dP_{in} as a function of P_{in} which rises gradually to a peak value of 43.6% at P_{in} = 0.8 W and decreases rapidly to zero from P_{in}~1.3-1.5W. The lower near-linear curve 1060 shows the variation in the laser wavelength as a function of P_{in}. The laser wavelength increases as P_{in} increases and $\Delta\lambda/\Delta P_{in}$ ~ 16 nm/W.

Figure 15 is a band-gap energy diagram for the cavity enhanced pumping gain mirror structure (CEP VECSEL) according to a second embodiment of the invention.

The spacings and composition of each layer of the gain mirror structure corresponding to Figure 15 are specified in the table of Figure 16. The spacings are calculated by dividing the required optical thickness by the refractive index of the layer material. The active region 3005 is 4.05 times $\lambda/2$ wide with λ=1050nm. The optical thickness is calculated from λ=1050nm rather than from the laser emission wavelength λ_L=1020nm for calibration purposes. The gain mirror structure of the CEP VECSEL is designed to be anti-resonant as it was for the first embodiment of the invention. The active region for the CEP VECSEL of this second embodiment of the invention is narrower than that for the first embodiment of the DP VECSEL of Figure 3.

The active region 3005 of Figure 15 contains six QWS 2010 arranged in three pairs. Each pair of QWs comprises a thin 10nm layer of AlGaAs sandwiched between two 7.5 nm layers of InGaAs and respective pairs are separated by a $\lambda/2$ layer at λ=1050nm of AlGaAs (x_{Al}=5%). Each pair of QWs is placed close to a maximum of the intra-cavity standing wave 2050.

The highly reflective Bragg stack 3015 is constructed from a repeating unit 2040 comprising eight alternating layers of AlAs and AlGaAs (x_{Al}=12%), including one $\lambda'/2$ layer of AlAs and 7 layers of optical thickness $\lambda'/4$. For this HR layer 3015 a design wavelength of λ'=927nm is used to ensure that the HR region has medium reflectivity at λ_P=820nm and high reflectivity at λ_L = 1020nm. The entire eight-layer unit is repeated ten times and a single additional $\lambda'/4$ layer of AlAs is added adjacent to the active region to contain the carriers within the active region. The HR region 3015 thus has a total of eighty-one layers.

The AR region 3025 consists of three alternating AlGaAs (x_{Al}=12%) / AlAs pairs of optical thickness $\lambda/4$, where λ=1050nm. Adjacent to these three pairs of layers is a structure comprising a $\lambda/4$ layer of AlAs, a $\lambda/2$ layer of AlGaAs (x_{Al}=12%) and a thin surface caping layer of GaAs. The optical thickness of the AlGaAs layer adjacent to the caping layer is reduced to accommodate the optical depth of the caping layer. The multi-layer structure of AR region 3025 is designed to give very low reflectivity at λ_L = 1020nm and medium reflectivity at λ_P = 820nm. The incoming pump light 3050 has energy greater than the band energy of the $Al_{0.05}Ga_{0.95}As$ of the active region but less than the band energy of the multi-layered structures of the HR

region 3015 and of the AR region 3025. The outgoing laser light 3055 at λ_L is reflected from the HR region. Since the AR region 3025 has medium reflectivity at λ_P, a portion of the pump light will be reflected back through the active region and a further portion will pass through the AR region 3025 and enter the air 3035 of the main laser cavity.

Figures 17 to 21 are predictions obtained from mathematical models of the CEP VECSEL structure of Figure 14.

Figure 17 shows the Bragg reflectivity as a function of the wavelength for the HR region 3015. Dispersion has not been taken into account in the model. The Bragg reflectivity has a first broad (~50nm wide) flat peak centred on the pump wavelength λ_P = 820nm and a second broad (~70nm wide) flat peak centred on the laser wavelength λ_L = 1020nm.

Figure 18 shows the Bragg reflectivity as a function of wavelength for the AR region 3025. The reflectivity is about 30% at λ_P = 820nm and approximately zero at λ_L = 1020nm. It is instructive to compare this with the reflectivity of the DP VECSEL of the first embodiment of the invention shown in Figure 5, where the reflectivity is approximately zero both at λ_P = 820nm and at λ_L = 1020nm.

Figure 19 shows the absorption efficiency and the reflectivity of the whole CEP VECSEL gain mirror according to the second embodiment of the invention. The solid curve 4010 is the absorption efficiency and the dashed curve 4020 is the reflectivity. The absorption efficiency has a peak centred on λ_P = 820nm and an adjacent peak at about 855nm.

Figures 20 and 21 show characteristics of the whole CEP VECSEL gain mirror according to the second embodiment of the invention. Dispersion is taken into account in this mathematical model but absorption is not. Figure 19 gives the reflectivity profile 4030 and the $|E|^2$ field distribution 4040 in the active region in the region of the pump wavelength 820nm. Figure 20 gives the reflectivity profile 4050 and the $|E|^2$ field distribution 4060 in the active region in the region of the laser wavelength 1020nm.

The $|E|^2$ distribution in the QWs in the region of the laser wavelength (Figure 20) has two overlapping peaks, the tails of which have merged to produce a broad

peak in $|E|^2$ centred on the laser wavelength. This will result in a larger effective gain bandwidth than that of the material gain itself.

From Figure 21 we see that the CEP VECSEL gain mirror structure is highly reflective at the pump wavelength. The $|E|^2$ distribution in this case has two narrow peaks that have relatively little overlap. One of the two peaks is centred on the pump wavelength.

References

[1] "Diode-pumped broadband Vertical-External-Cavity surface Emitting semiconductor laser: Application to high sensitivity intracavity laser absorption spectroscopy", A. Garnache et al., JOSA B, September 2000

CLAIMS

1. A vertical cavity laser device comprising:

a multi-layer laser structure having a pump light receiving face for receiving incident pump light at a pump wavelength, and a semiconductor gain region operable to provide optical gain at a laser emission wavelength in response to the pump light;

two laser cavity mirrors disposed about the multi-layer laser structure so as to define a laser cavity wherein each laser cavity mirror is operable to reflect light at the laser emission wavelength; and

a pump mirror disposed behind the gain region so as to reflect pump light back through the gain region for at least a second pass.

2. A device according to claim 1, comprising an anti-reflection coating at the pump light receiving face, wherein said anti-reflection coating is operable to reduce reflections at the pump wavelength.

3. A device according to claim 2, wherein said anti-reflection coating has substantially zero reflectivity at the pump wavelength and substantially zero reflectivity at the laser emission wavelength.

4. A device according to claim 1, comprising a further pump-mirror structure on the pump light receiving face operable to create a sub-cavity to promote multiple passes of pump light through said gain region.

5. A device according to claim 4, wherein said further pump mirror has a reflectivity in the range 10% to 60% at the pump wavelength and substantially zero reflectivity at the laser emission wavelength.

6. A device according to claim 4 wherein said further pump mirror has a reflectivity of substantially 30% at the pump wavelength and substantially zero reflectivity at the laser emission wavelength.

7. A device according to any one of the above claims, wherein at least one of said cavity-mirrors is disposed with respect to the multi-layer lasing structure so as to define an external laser cavity.

8. A device according to any one of the above claims, comprising an optical pump source arranged to supply the pump light to the pump light receiving face.

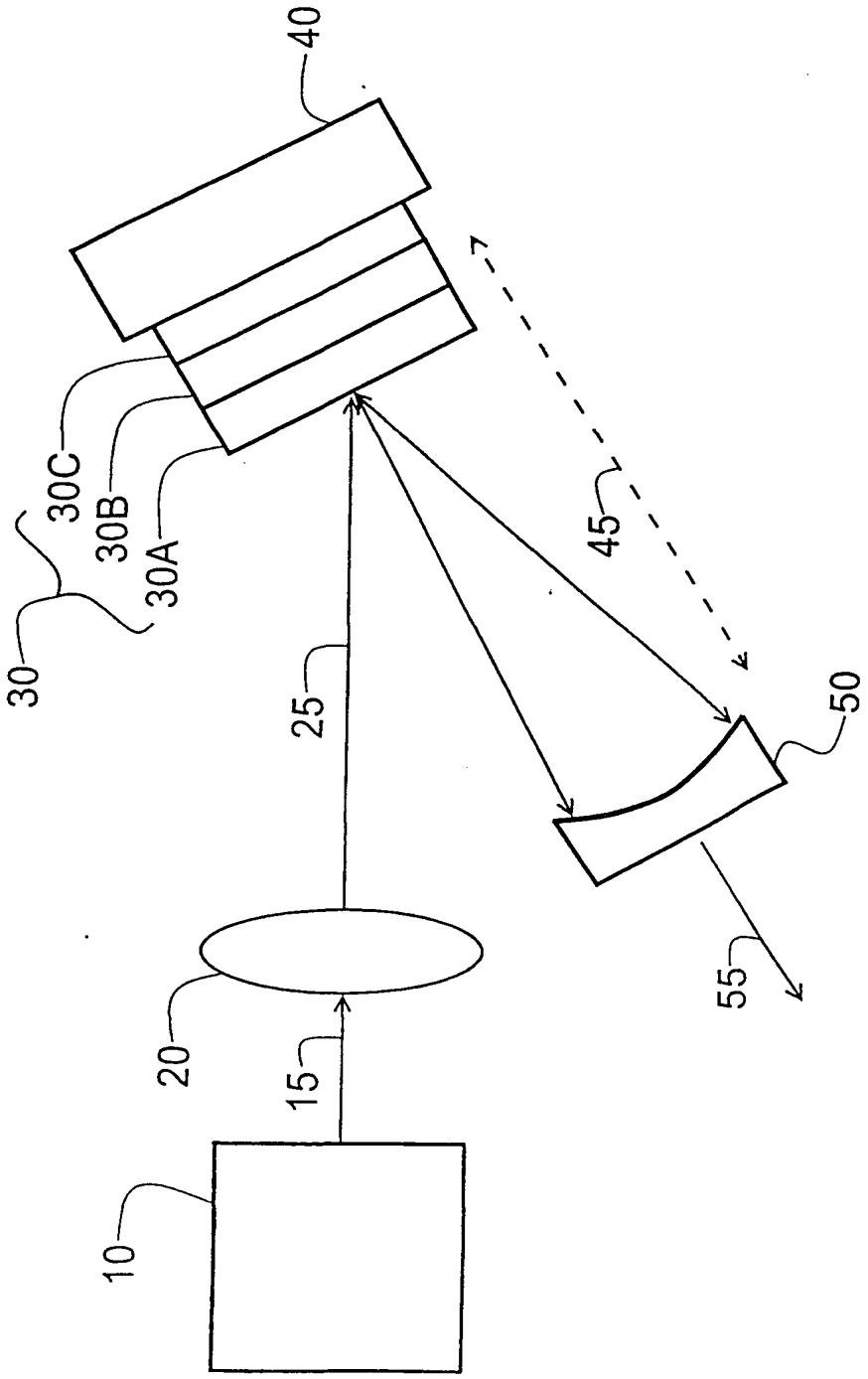

Fig. 1

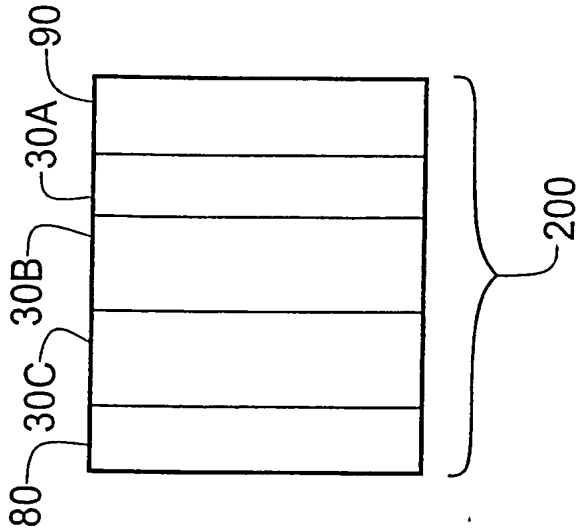

Fig. 2B

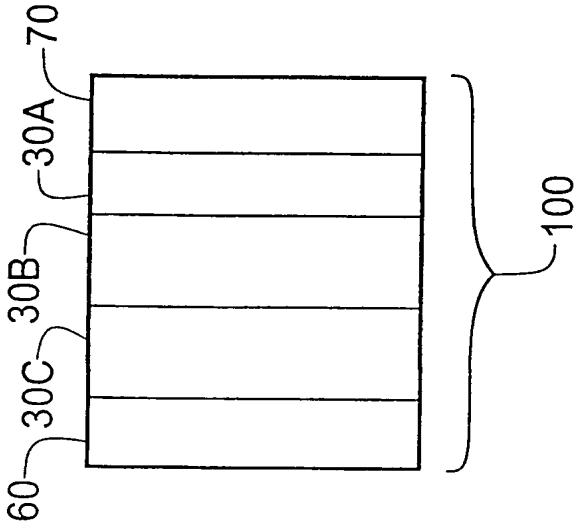

Fig. 2A

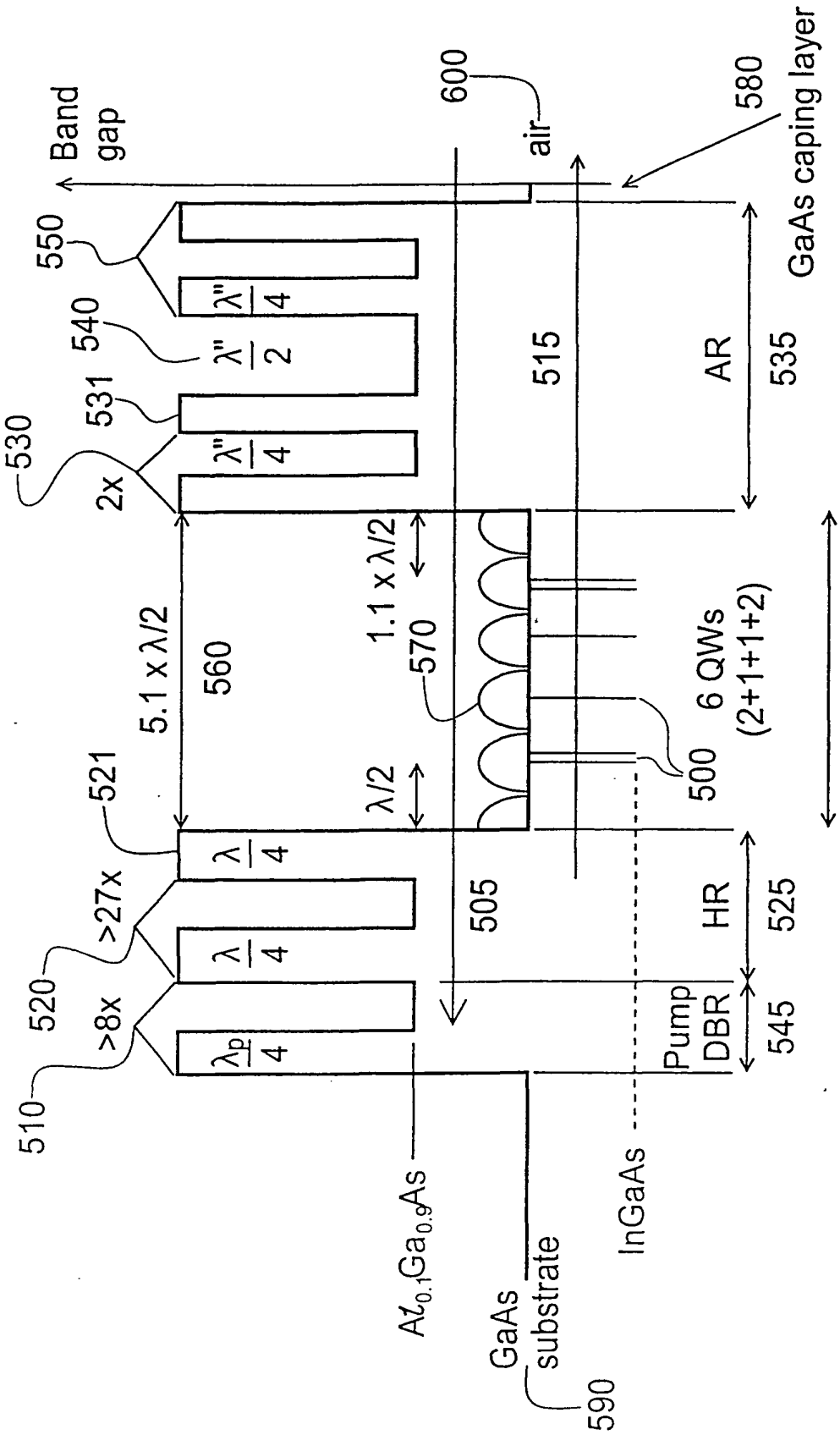
Band gap
600
air
580
GaAs caping layer
550
540
531
530
2x
λ"/4
λ"/2
λ"/4
515
AR
535
1.1 x λ/2
570
5.1 x λ/2
560
6 QWs (2+1+1+2)
505
500
λ/2
521
λ/4
>27x
520
λ/4
>8x
λp/4
510
505
HR
525
Pump DBR
545
Al0.1Ga0.9As
InGaAs
GaAs substrate
590

Fig. 3

Description	Material	Spacing (x10^{-9}m)
surface	GaAs	10
AR-~λ"/4	AlAs	64.7
AR-λ"/4	AlGaAs	65.4
AR-λ"/4	AlAs	76.5
AR-λ"/2	AlGaAs	130.9
AR-λ"/4	AlAs	76.5
AR-λ"/4 (x2)	AlGaAs	65.4
AR-λ"/4	AlAs	76.5
	..(x2)..	
ZA-1.1xλ/2	GaAs	?
ZA-2xQWs	InGaAs	8+10+8?
ZA-λ/2	GaAs	?
ZA-1xQWs	InGaAs	8?
ZA-λ/2	GaAs	?
ZA-1xQWs	InGaAs	8?
ZA-λ/2	GaAs	?
ZA-2xQWs	InGaAs	8+10+8?
ZA-λ/2	GaAs	?
Bragg 1 HR-λ/4	AlAs (x27)	86.4
Bragg 1 HR-λ/4	AlGaAs	73.9
Bragg 1 HR-λ/4	AlAs	86.4
	..	
Bragg 2 pump DBR-λp/4	AlGaAs	56.8
Bragg 2 pump DBR-λp/4	AlAs	69.5
	....(>8x)....	

Fig. 4

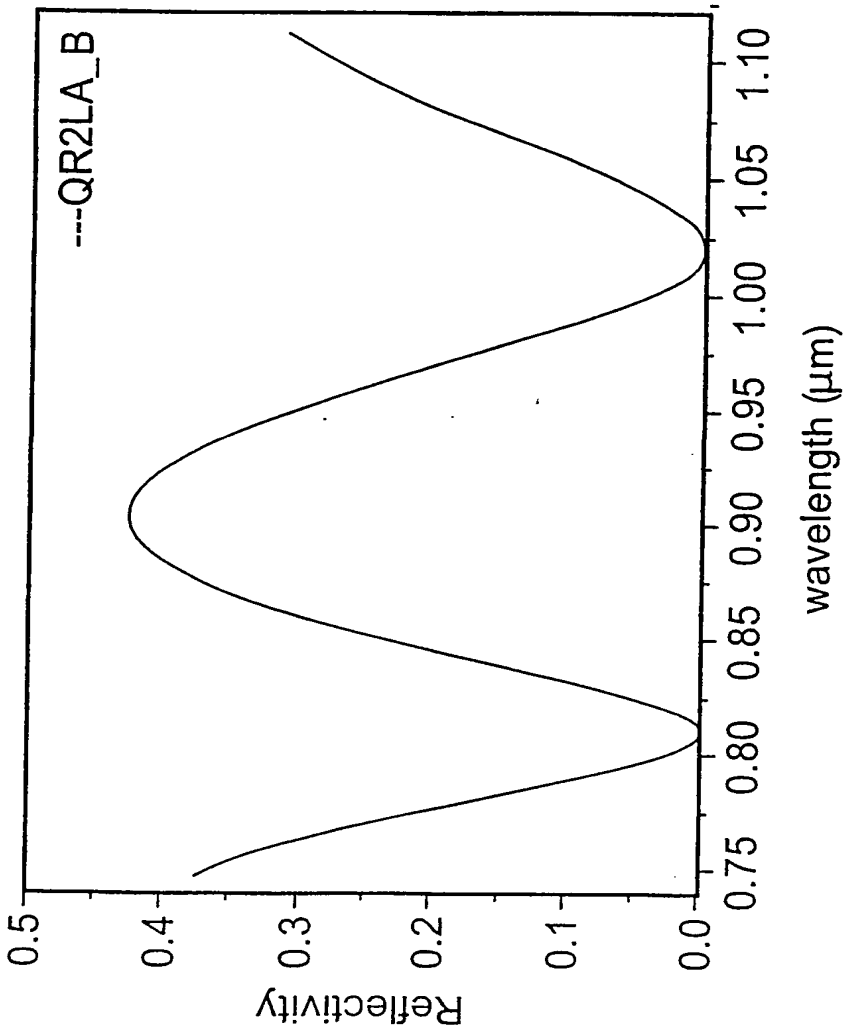
---QR2LA_B
Reflectivity
0.0
0.1
0.2
0.3
0.4
0.5
0.75
0.80
0.85
0.90
0.95
1.00
1.05
1.10
wavelength (µm)

Fig. 5

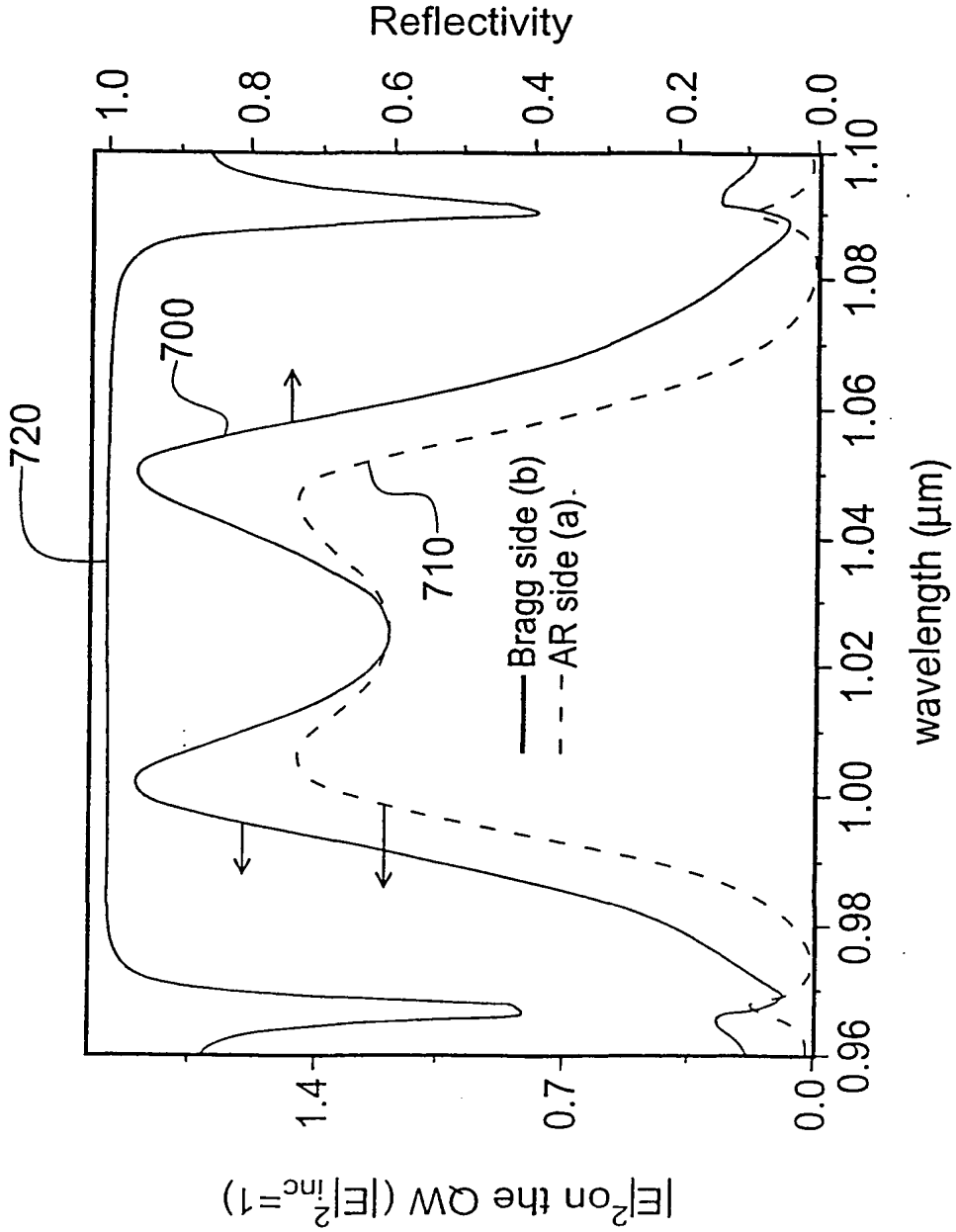

Fig. 6

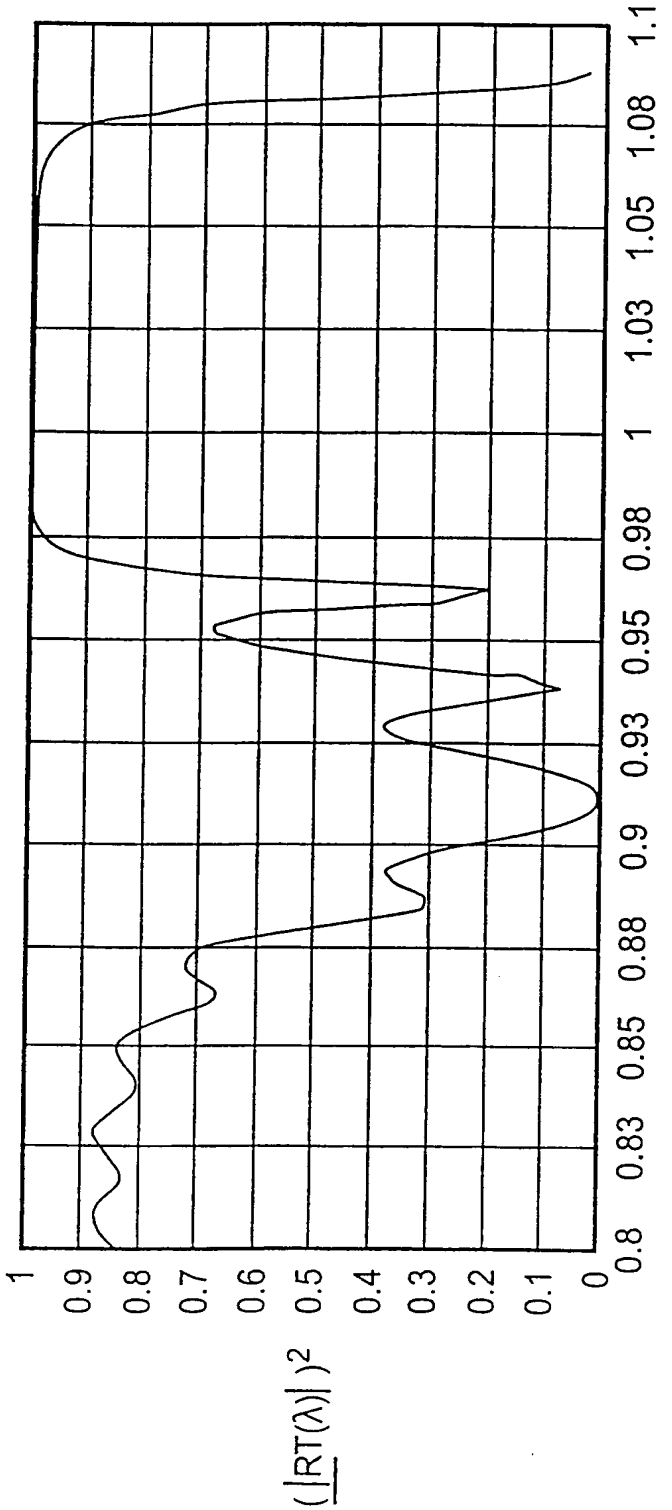
1
0.9
0.8
0.7
0.6
0.5
0.4
0.3
0.2
0.1
0
$(|RT(\lambda)|)^2$
0.8
0.83
0.85
0.88
0.9
0.93
0.95
0.98
1
1.03
1.05
1.08
1.1
λ

Fig. 7

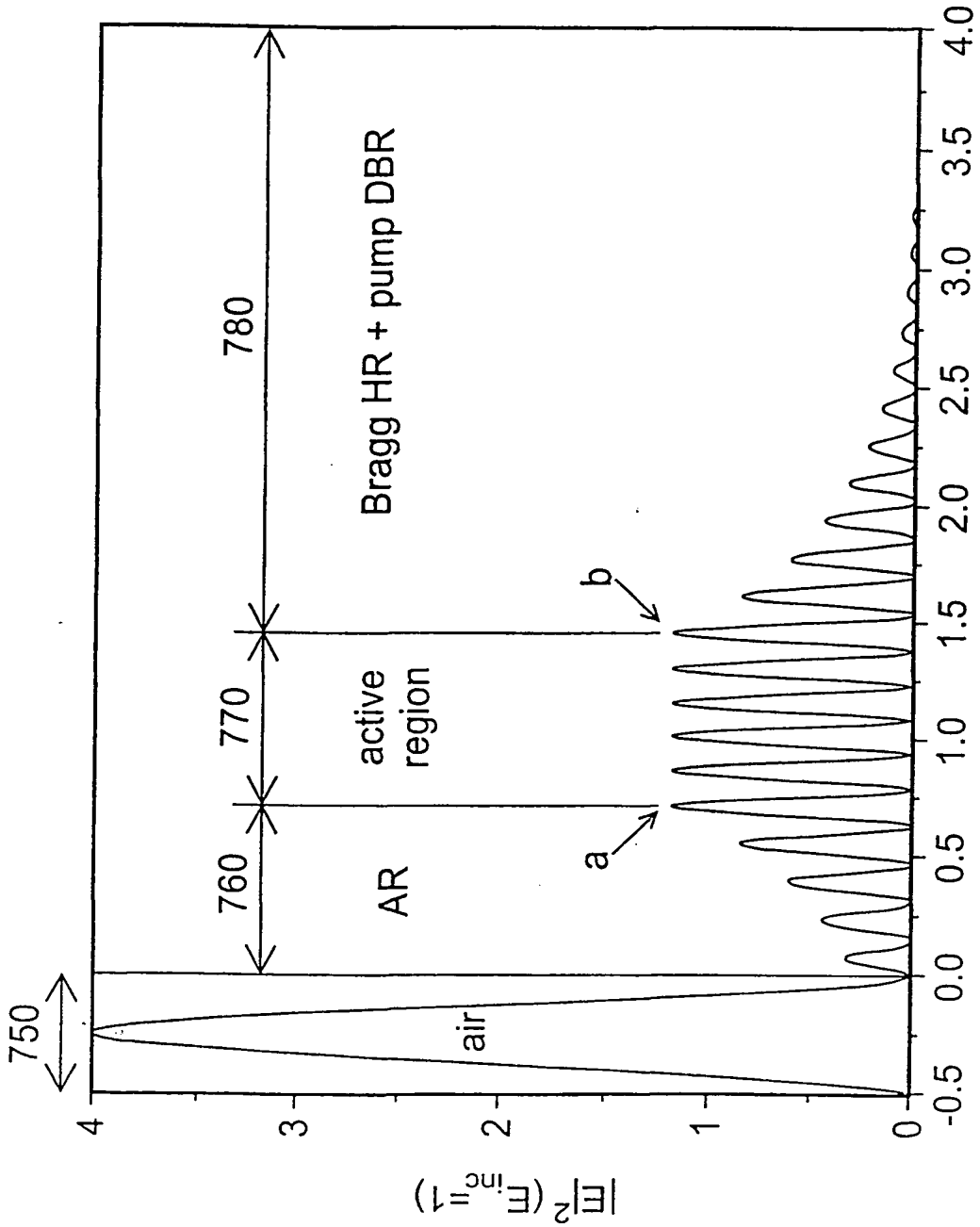
750
air
760
AR
770
active region
780
Bragg HR + pump DBR
a
b
$|E|^2$ (E_{inc}=1)
depth (μm)
4
3
2
1
0
-0.5
0.0
0.5
1.0
1.5
2.0
2.5
3.0
3.5
4.0

Fig. 8

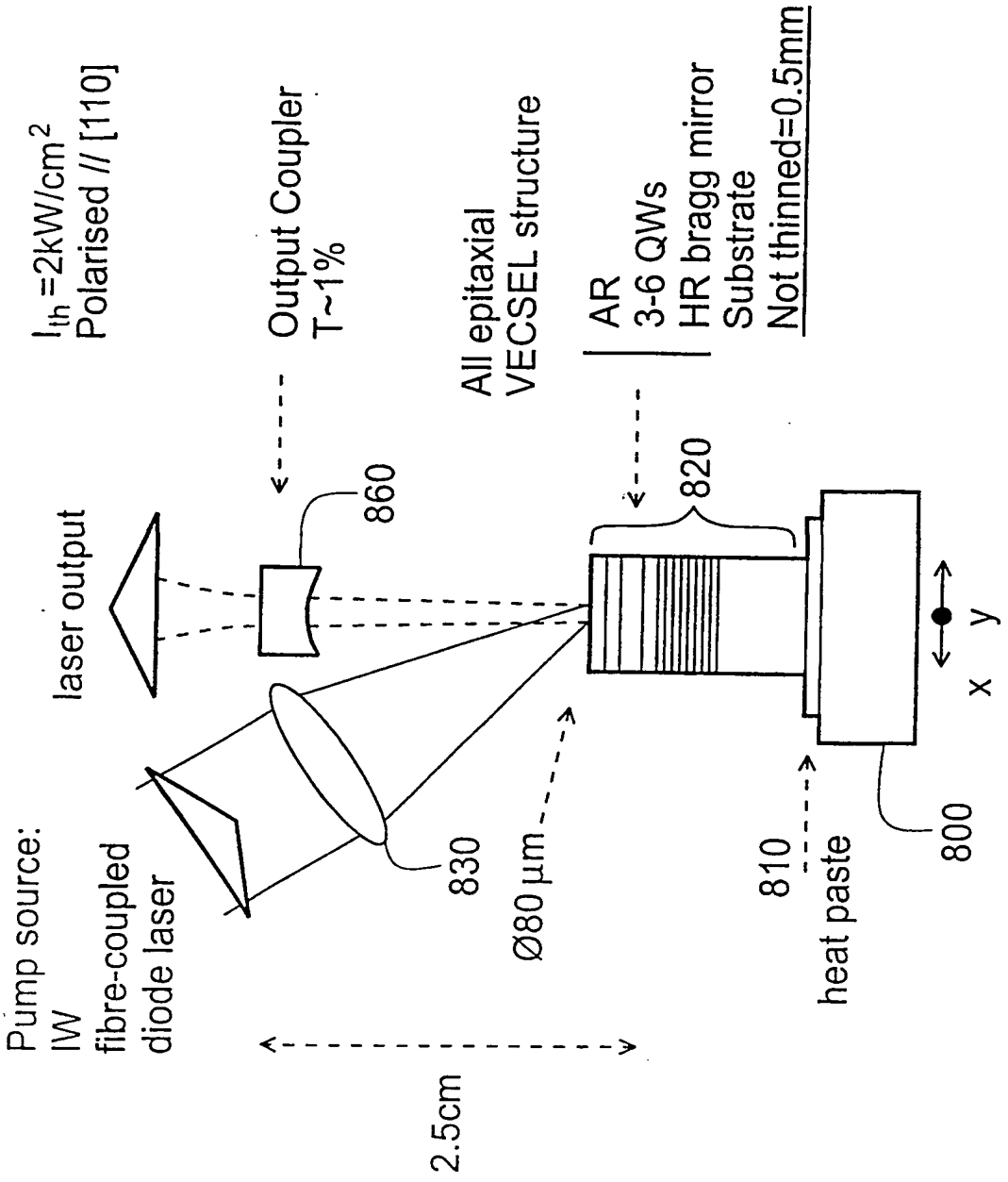

Fig. 9

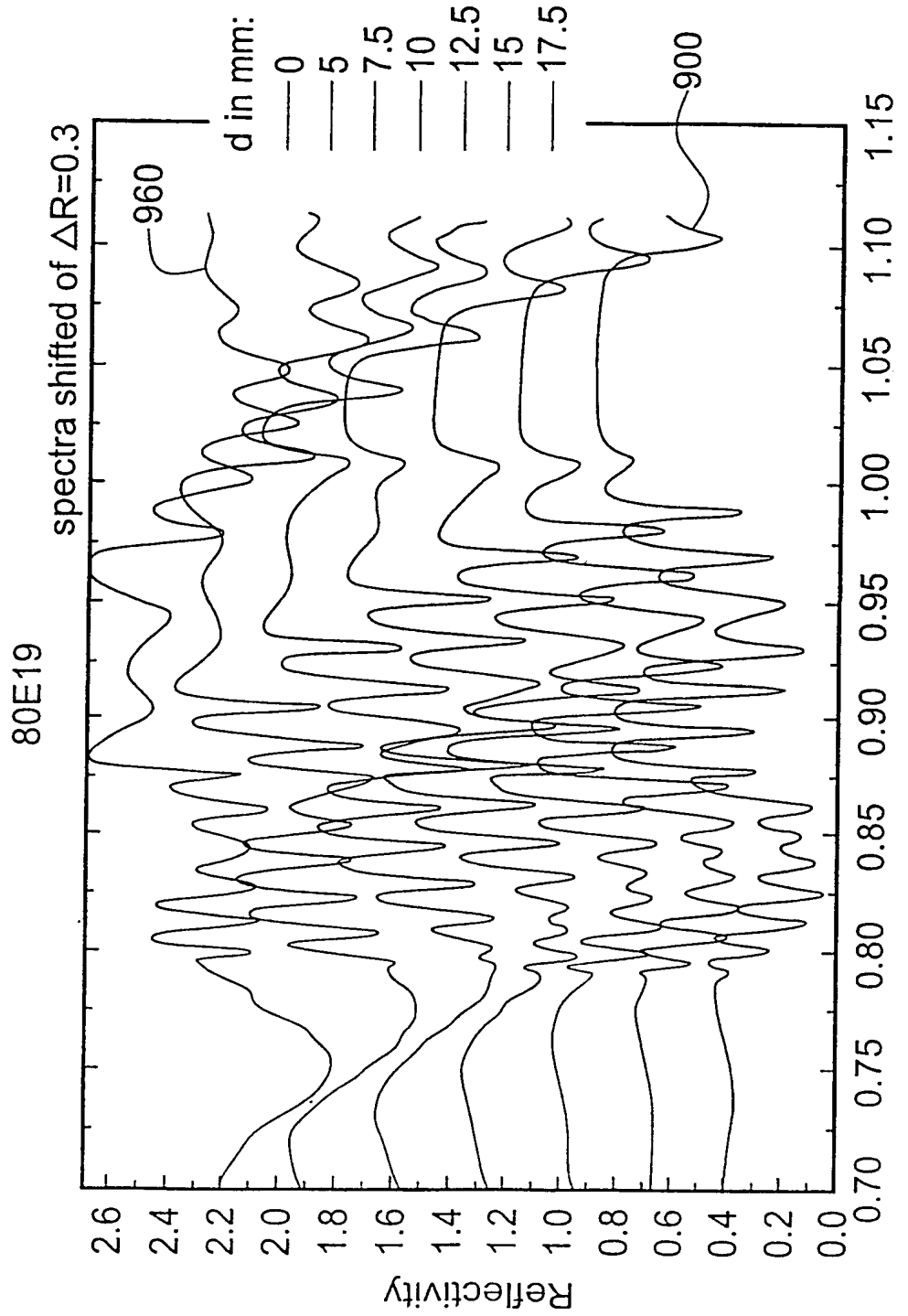

Fig. 10

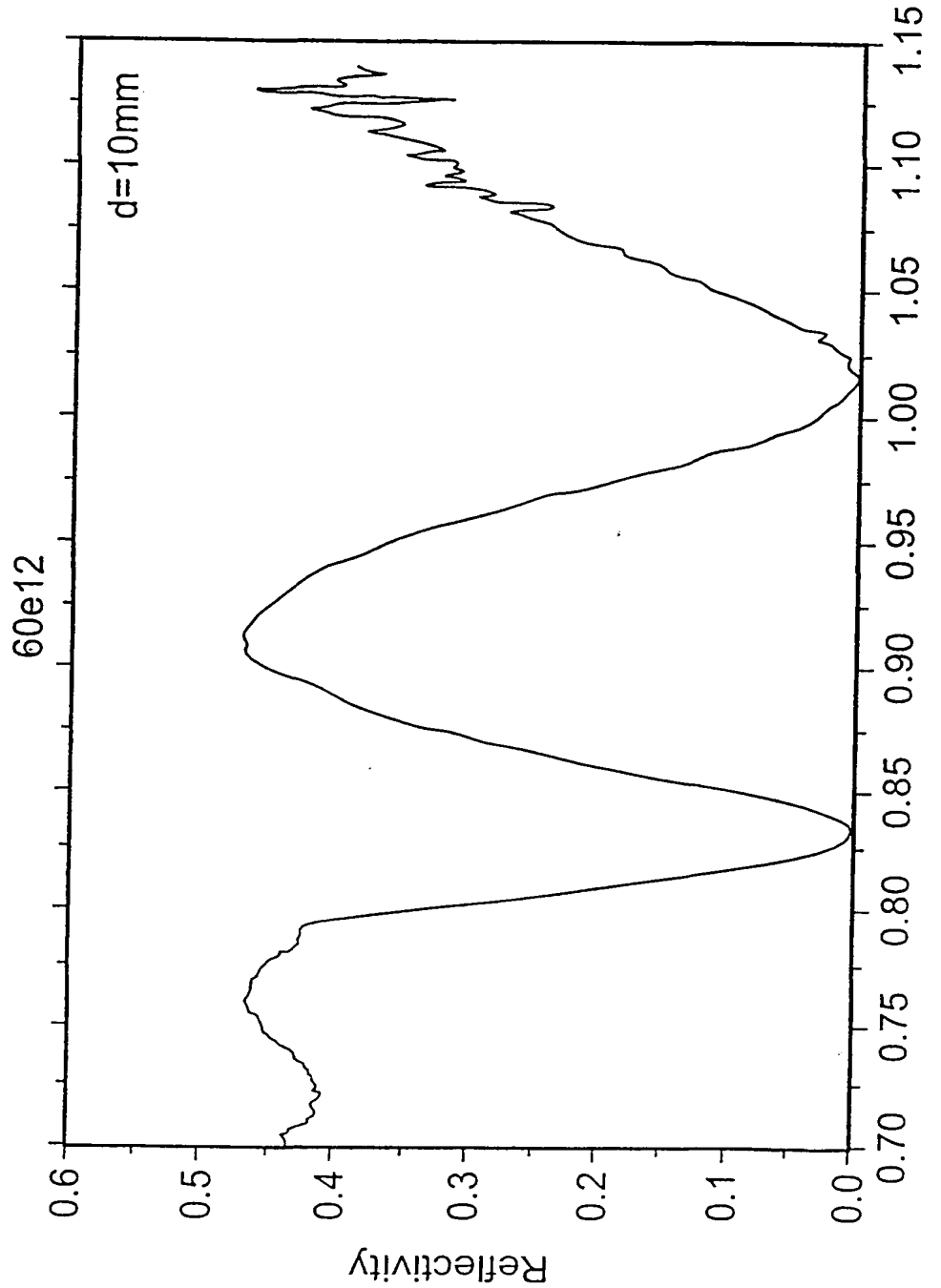
60e12
d=10mm
Reflectivity
0.0
0.1
0.2
0.3
0.4
0.5
0.6
0.70
0.75
0.80
0.85
0.90
0.95
1.00
1.05
1.10
1.15
wavelength (µm)

Fig. 11

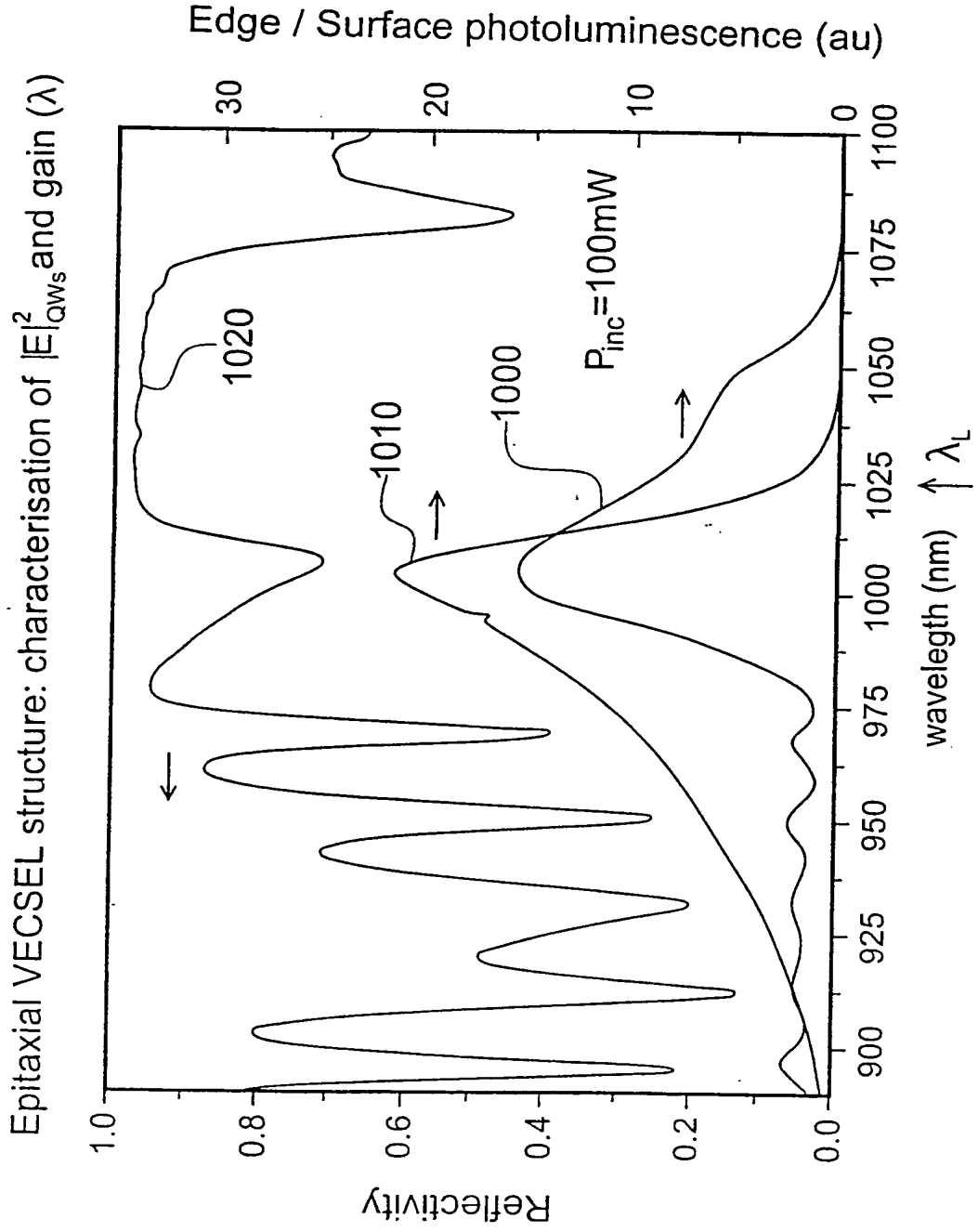
Edge / Surface photoluminescence (au)
Epitaxial VECSEL structure: characterisation of $|E|^2_{QWs}$ and gain (λ)
Reflectivity
wavelegth (nm) ↑ λ_L
1020
1010
1000
P_{inc}=100mW

Fig. 12

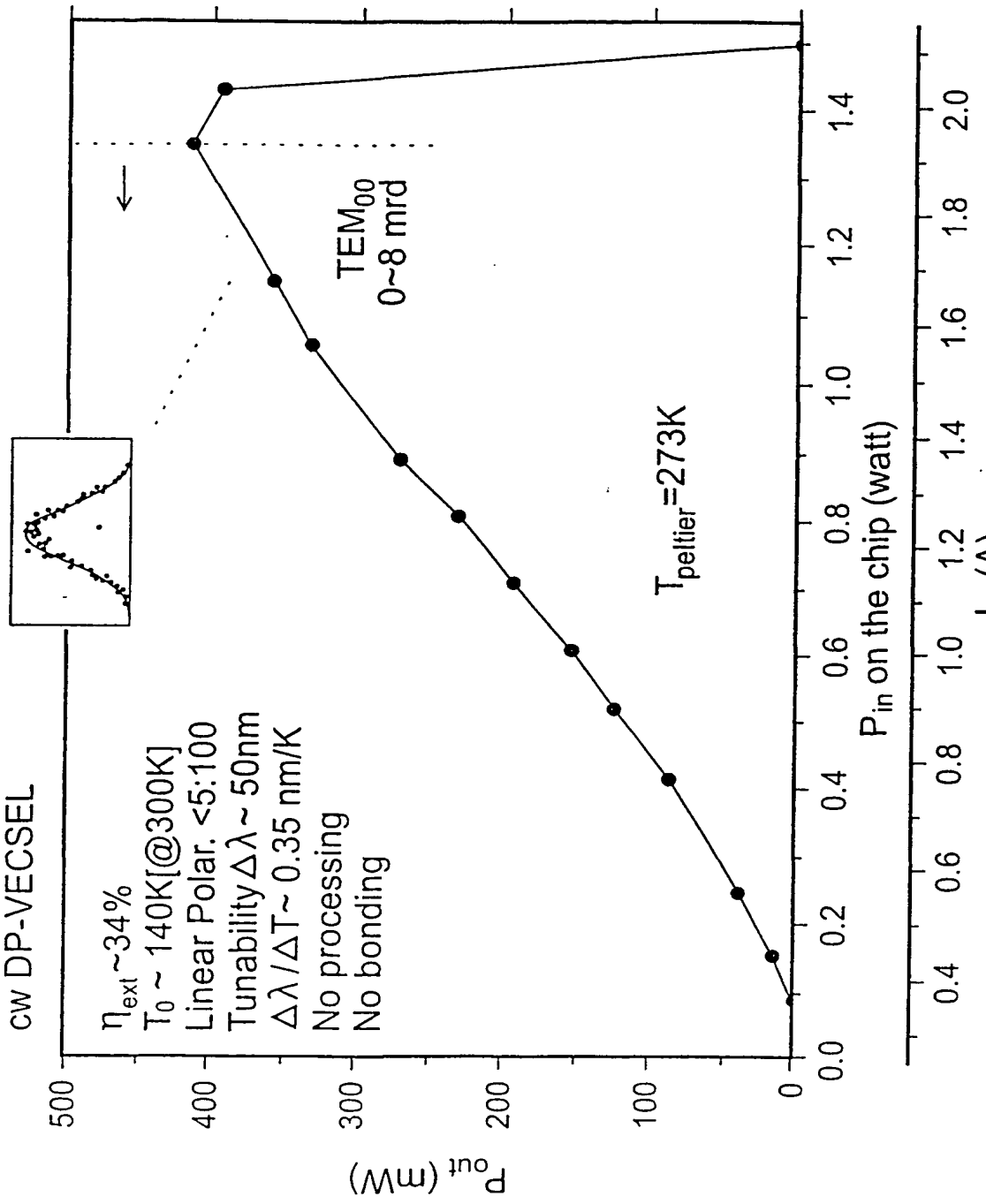

Fig. 13

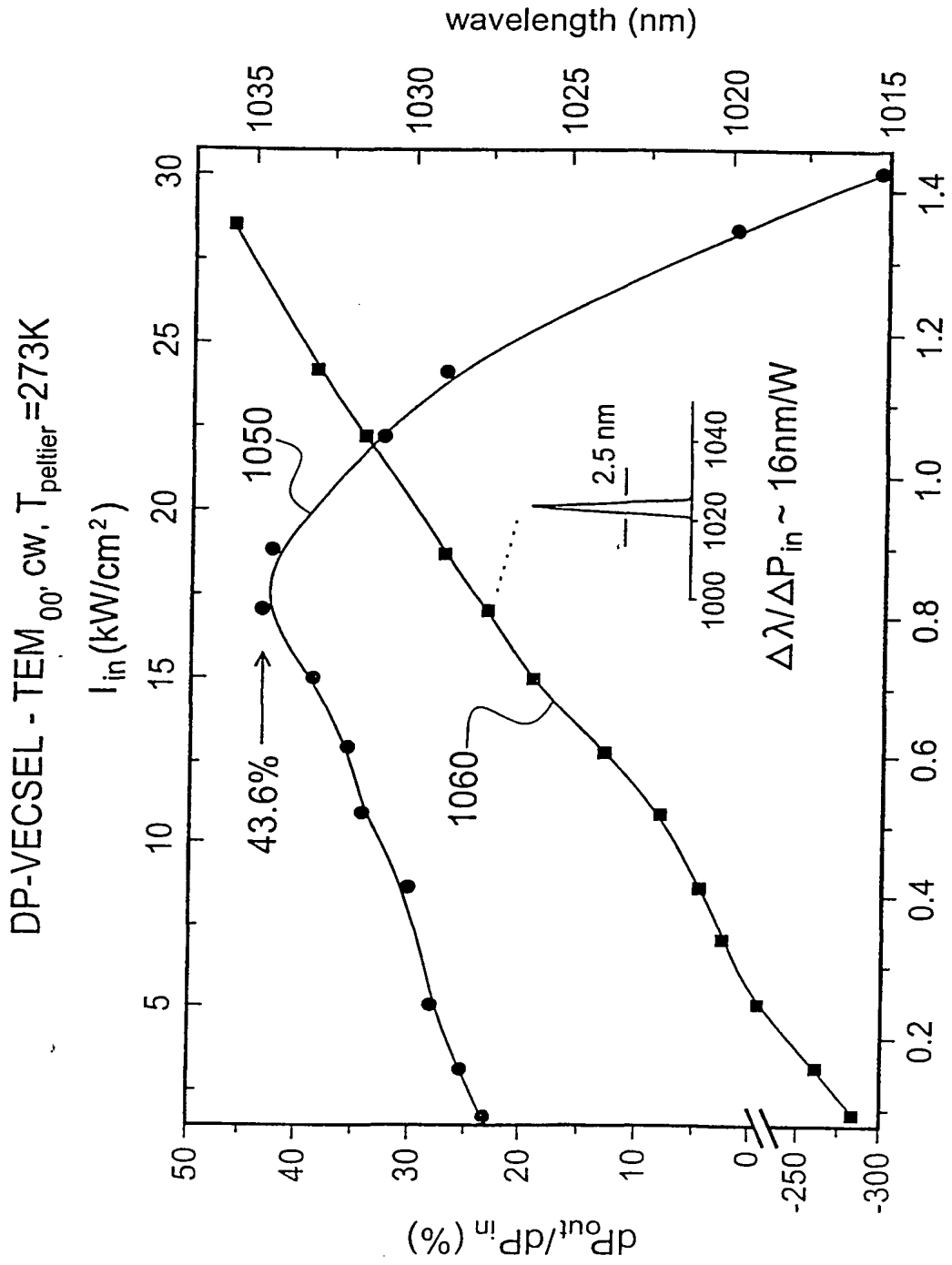
wavelength (nm)
1035
1030
1025
1020
1015
DP-VECSEL - TEM00, cw, Tpeltier=273K
Iin(kW/cm2)
30
25
20
15
10
5
1050
43.6%
1060
2.5 nm
1000 1020 1040
Δλ/ΔPin ~ 16nm/W
1.4
1.2
1.0
0.8
0.6
0.4
0.2
Pin on the chip (watt)
dPout/dPin (%)
50
40
30
20
10
0
-250
-300

Fig. 14

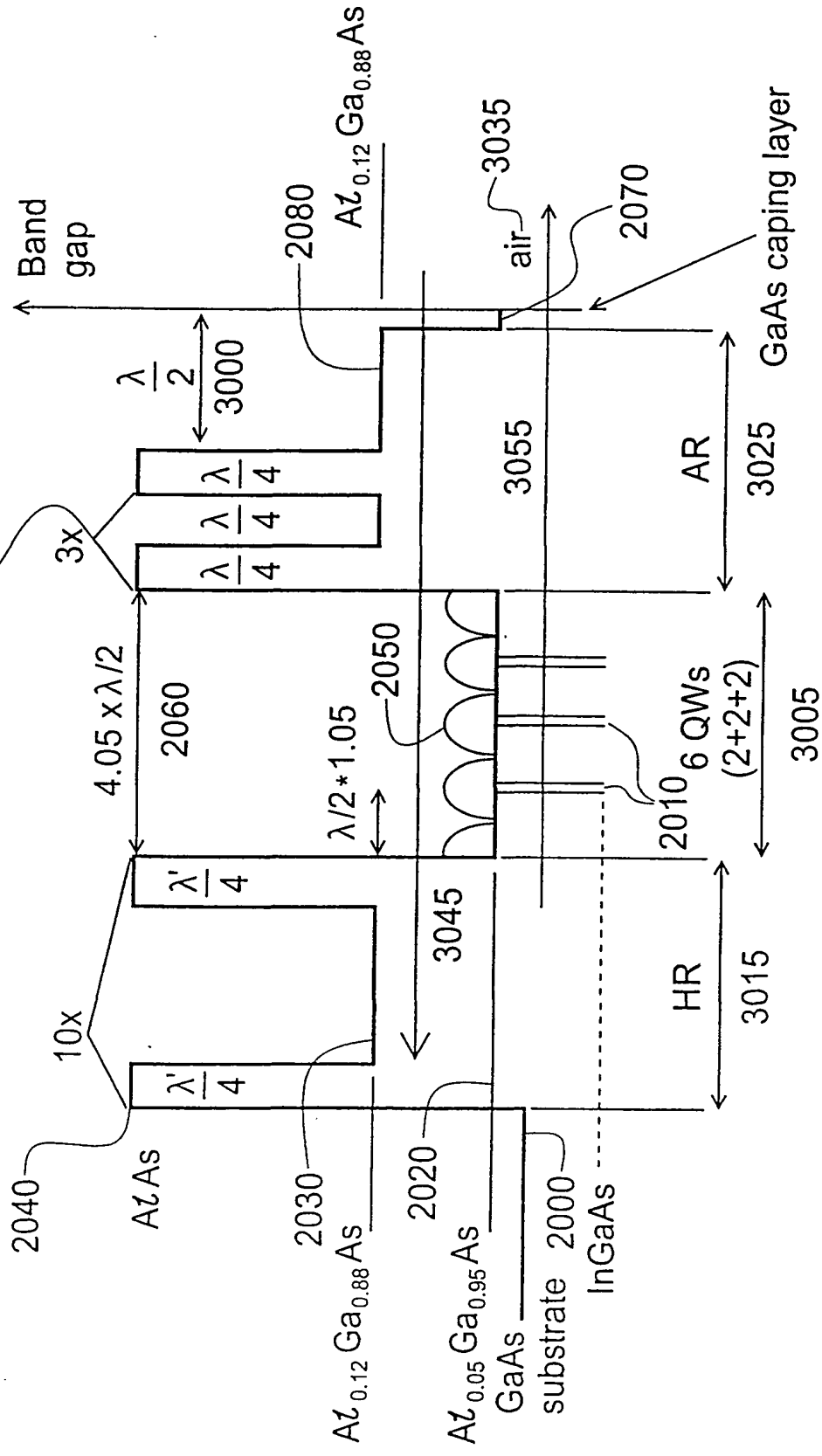

Fig. 15

Thickness:(Surface to substrate)

Description	Composition	Thickness(nm)	#
surface	GaAs	10	1
AR*-~λ/2	Al GaAs(x_{Al}=12%)	138.28	2
AR-λ/4	Al As	89.34	3
AR-λ/4	Al GaAs(x_{Al}=12%)	79.24	4
AR-λ/4	Al As	89.34	5
(λ=1050nm)	..(x3)..		
ZA-xλ/2 (λ=1050nm) .	Al GaAs(x_{Al}=5%)	138.6	10
ZA-2xQWs	InGaAs/Al GaAs/InGaAs(n_{ingaas}~3.6)	7.5/10/7.5	11-13
ZA-λ/2	Al GaAs(x_{Al}=5%)	125.82	14
ZA-2xQWs	InGaAs/Al GaAs/InGaAs	7.5/10/7.5	15-17
ZA-λ/2	Al GaAs(x_{Al}=5%)	125.82	18
ZA-2xQWs	InGaAs/Al GaAs/InGaAs	7.5/10/7.5	19-21
ZA-λ/2	Al GaAs(x_{Al}=5%)	146.17	22
Bragg HR-λ'/4	Al As	79.09	23
Bragg HR-λ'/4	Al GaAs(x_{Al}=12%)	67.69	24
Bragg HR-λ'/4	Al As	79.09	25
Bragg HR-λ'/4	Al GaAs(x_{Al}=12%)	67.69	26
Bragg HR-λ'/2	Al As	158.18	27
Bragg HR-λ'/4	Al GaAs(x_{Al}=12%)	67.69	28
Bragg HR-λ'/4	Al As	79.09	29
Bragg HR-λ'/4	Al GaAs(x_{Al}=12%)	67.69	30
Bragg HR-λ'/4	Al As	79.09	31
.	..(x10)..		

Fig. 16

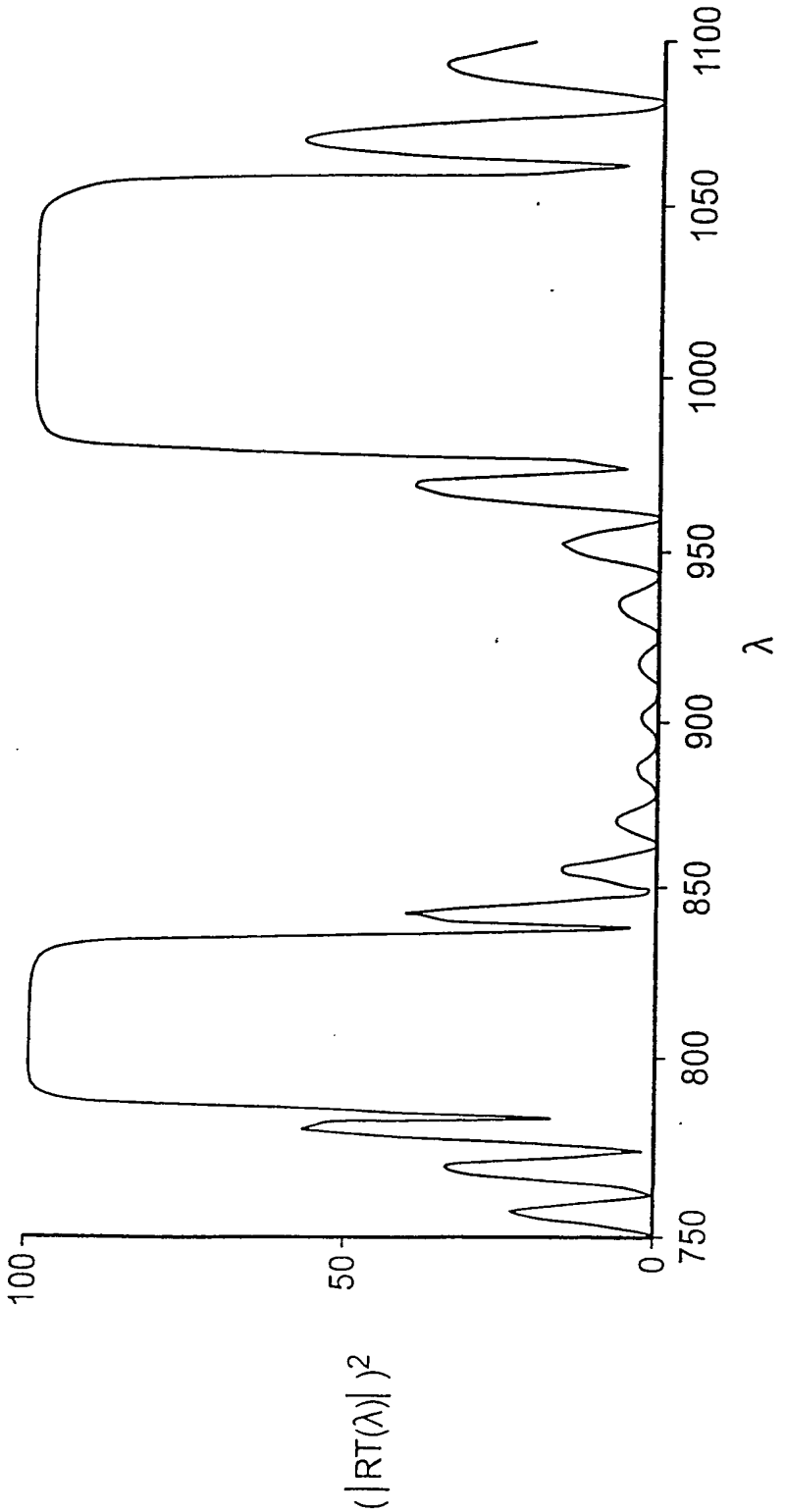

Fig. 17

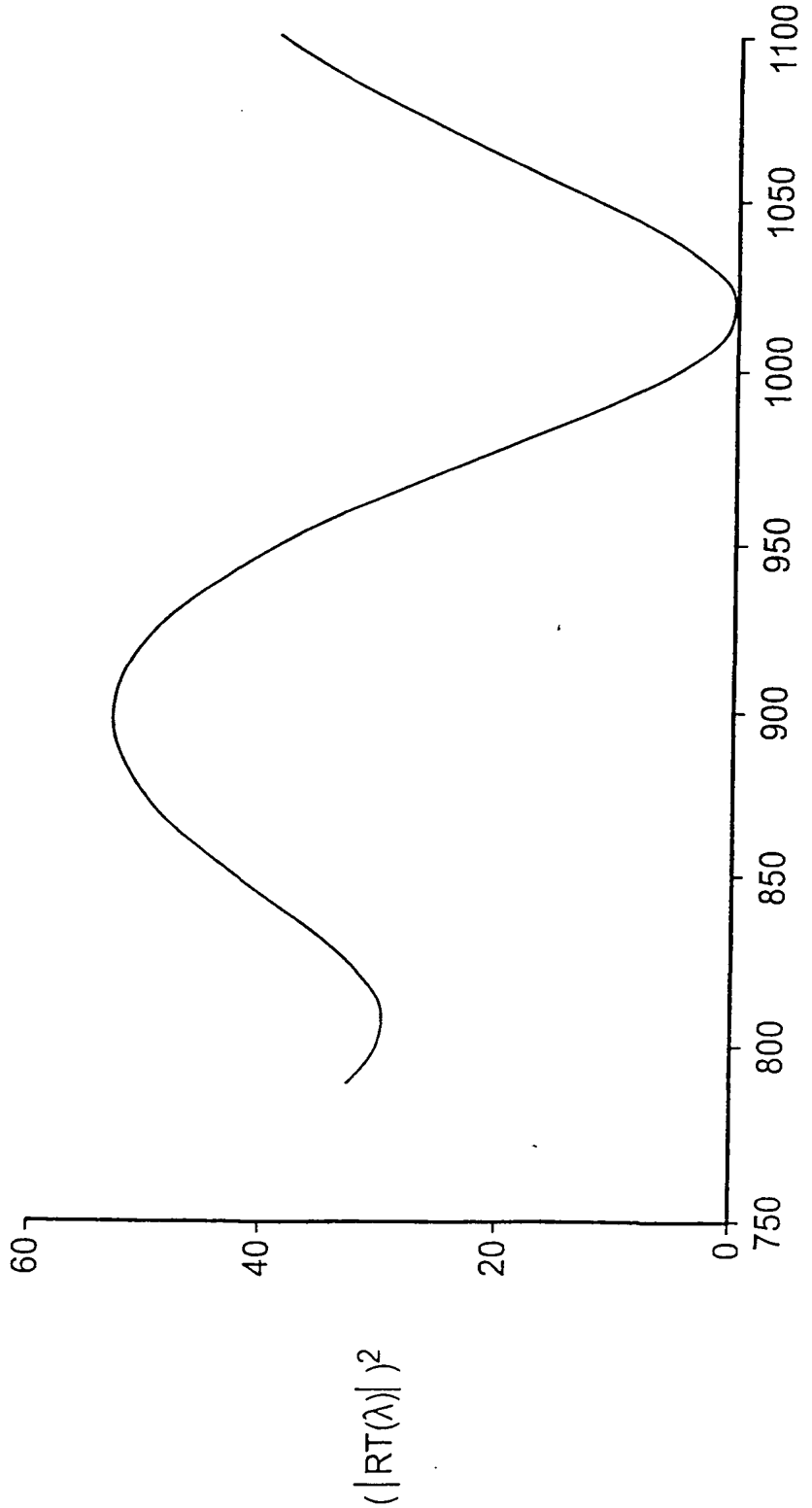

Fig. 18

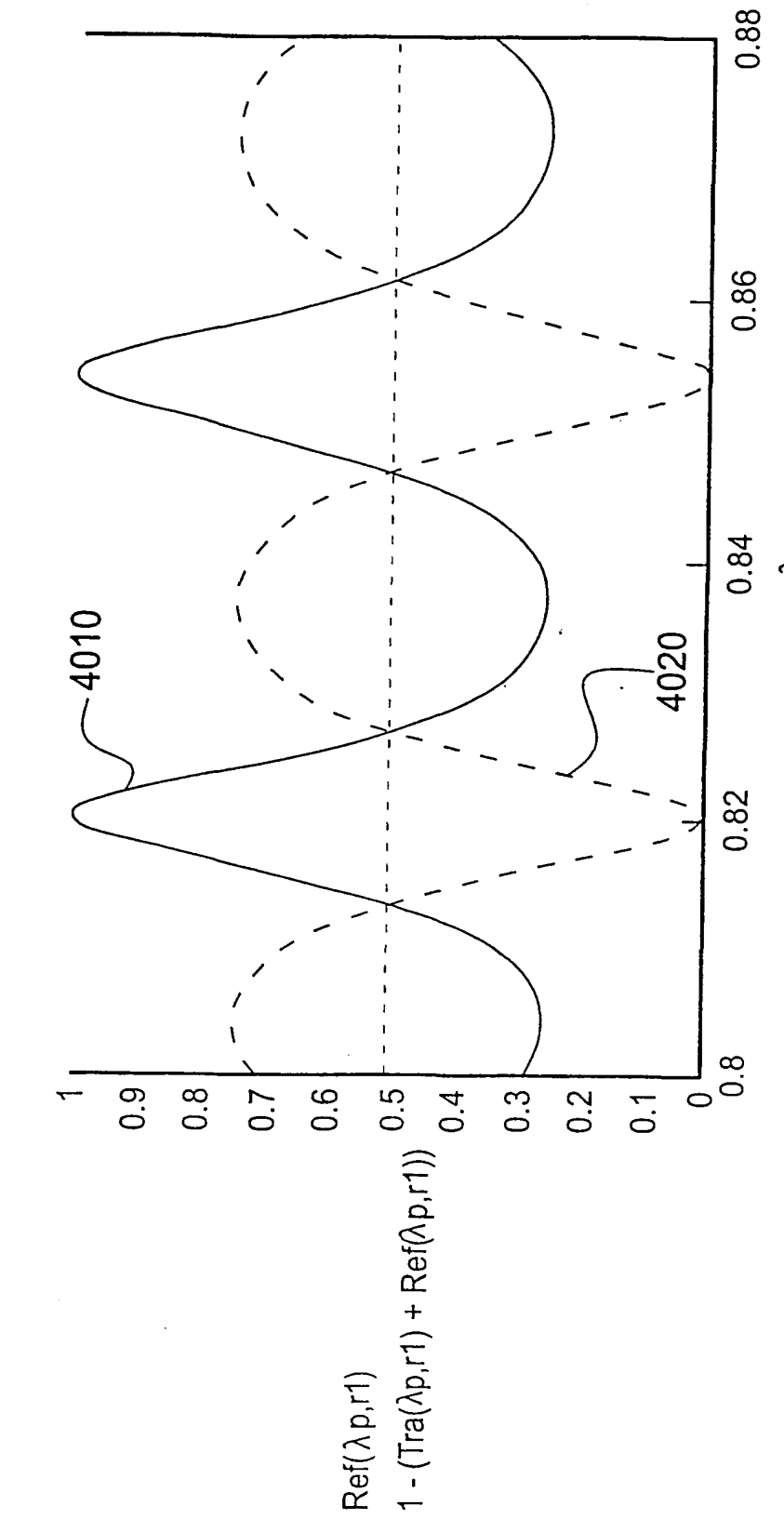
4010
4020
Ref(λp,r1)
1 - (Tra(λp,r1) + Ref(λp,r1))
λp / 10^-4
0.8
0.82
0.84
0.86
0.88
0
0.1
0.2
0.3
0.4
0.5
0.6
0.7
0.8
0.9
1

Fig. 19

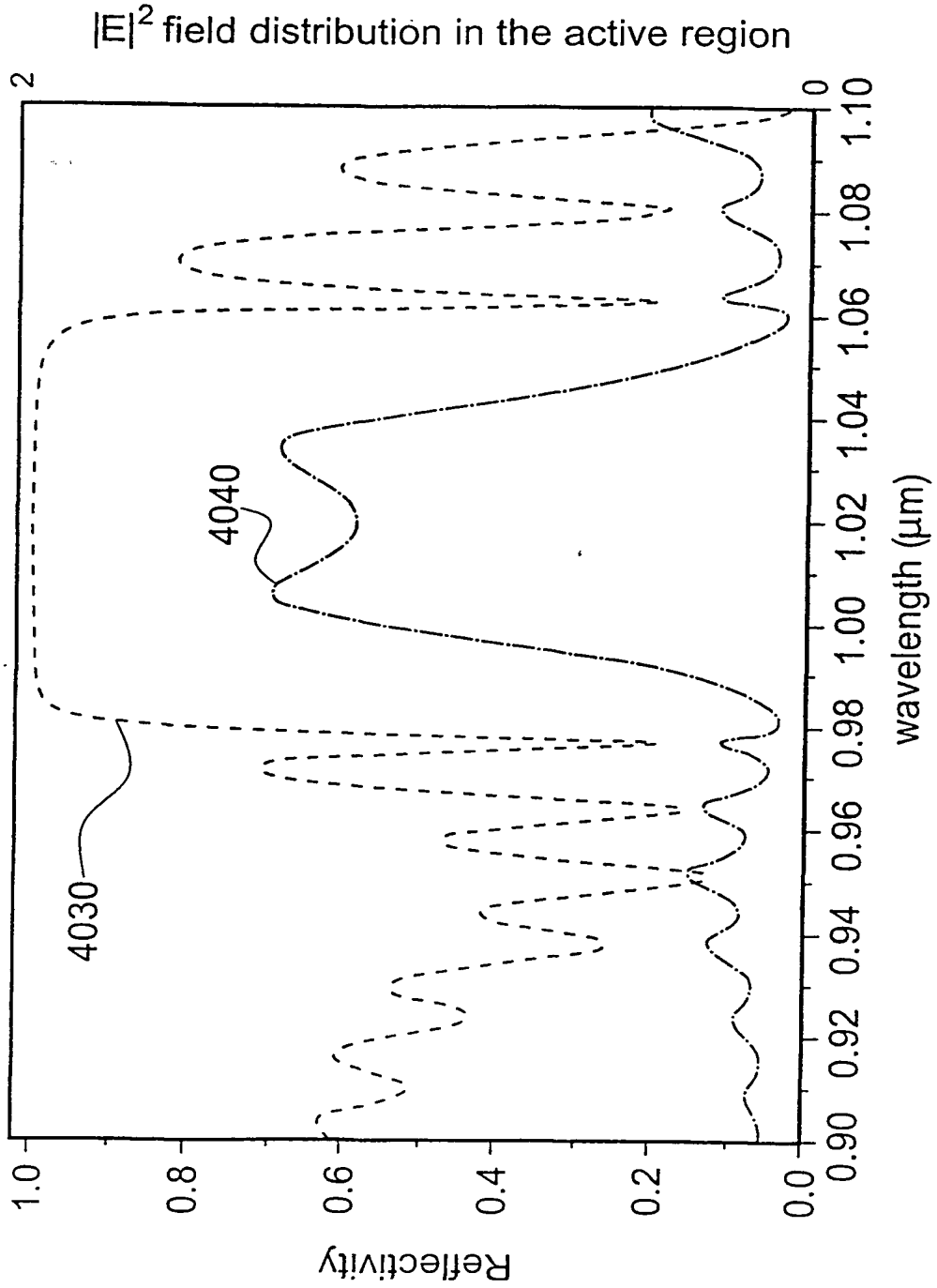
$|E|^2$ field distribution in the active region
2
0
1.10
1.08
1.06
1.04
1.02
1.00
0.98
0.96
0.94
0.92
0.90
wavelength (μm)
4040
4030
1.0
0.8
0.6
0.4
0.2
0.0
Reflectivity

Fig. 20

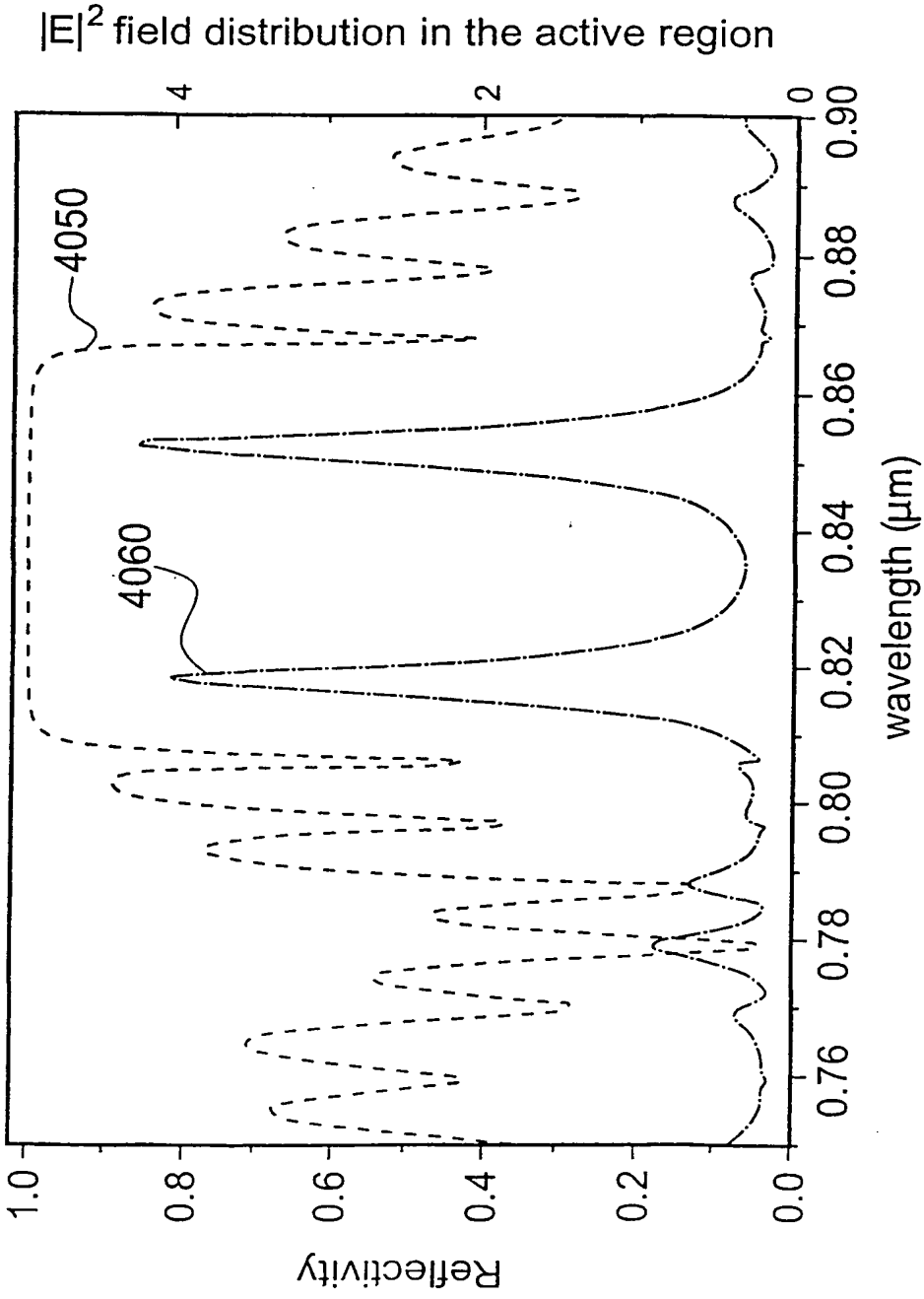
$|E|^2$ field distribution in the active region
4050
4060
Reflectivity
wavelength (μm)
0.0
0.2
0.4
0.6
0.8
1.0
0.76
0.78
0.80
0.82
0.84
0.86
0.88
0.90
0
2
4

Fig. 21

INTERNATIONAL SEARCH REPORT

PCT/GB 01/05387

A. CLASSIFICATION OF SUBJECT MATTER
IPC 7 H01S5/183 H01S5/04

According to International Patent Classification (IPC) or to both national classification and IPC

B. FIELDS SEARCHED

Minimum documentation searched (classification system followed by classification symbols)
IPC 7 H01S

Documentation searched other than minimum documentation to the extent that such documents are included in the fields searched

Electronic data base consulted during the international search (name of data base and, where practical, search terms used)
EPO-Internal, WPI Data, PAJ, IBM-TDB, INSPEC, COMPENDEX

C. DOCUMENTS CONSIDERED TO BE RELEVANT

Category °	Citation of document, with indication, where appropriate, of the relevant passages	Relevant to claim No.
Y	WO 00 10234 A (COHERENT INC) 24 February 2000 (2000-02-24) page 7, line 1 -page 9, line 24 page 11, line 10 -page 12, line 3 page 15, line 22-29; figures 1-3 ---	1-8
Y	WO 99 12235 A (MICRON OPTICS INC) 11 March 1999 (1999-03-11) page 12, line 22 -page 14, line 23 --- -/--	1-8

[X] Further documents are listed in the continuation of box C.

[X] Patent family members are listed in annex.

° Special categories of cited documents :

"A" document defining the general state of the art which is not considered to be of particular relevance

"E" earlier document but published on or after the international filing date

"L" document which may throw doubts on priority claim(s) or which is cited to establish the publication date of another citation or other special reason (as specified)

"O" document referring to an oral disclosure, use, exhibition or other means

"P" document published prior to the international filing date but later than the priority date claimed

"T" later document published after the international filing date or priority date and not in conflict with the application but cited to understand the principle or theory underlying the invention

"X" document of particular relevance; the claimed invention cannot be considered novel or cannot be considered to involve an inventive step when the document is taken alone

"Y" document of particular relevance; the claimed invention cannot be considered to involve an inventive step when the document is combined with one or more other such documents, such combination being obvious to a person skilled in the art.

"&" document member of the same patent family

Date of the actual completion of the international search	Date of mailing of the international search report
4 February 2002	12/02/2002

Name and mailing address of the ISA	Authorized officer
European Patent Office, P.B. 5818 Patentlaan 2 NL - 2280 HV Rijswijk Tel. (+31-70) 340-2040, Tx. 31 651 epo nl, Fax: (+31-70) 340-3016	Gnugesser, H

Form PCT/ISA/210 (second sheet) (July 1992)

C.(Continuation) DOCUMENTS CONSIDERED TO BE RELEVANT

Category °	Citation of document, with indication, where appropriate, of the relevant passages	Relevant to claim No.
Y	FELIX C L ET AL: "HIGH-EFFICIENCY MIDINFRARED W LASER WITH OPTICAL PUMPING INJECTION CAVITY" APPLIED PHYSICS LETTERS, AMERICAN INSTITUTE OF PHYSICS. NEW YORK, US, vol. 75, no. 19, 8 November 1999 (1999-11-08), pages 2876-2878, XP000875952 ISSN: 0003-6951 abstract	1,4-6,8
Y	US 5 365 539 A (MOORADIAN ARAM) 15 November 1994 (1994-11-15) column 5, line 30-35; figures 6A,,6B	1,4-6,8
A	KUZNETSOV M ET AL: "HIGH-POWER (0.5-W CW) DIODE-PUMPED VERTICAL-EXTERNAL-CAVITY SURFACE-EMITTING SEMICONDUCTOR LASERS WITH CIRCULAR TEMOO BEAMS" IEEE PHOTONICS TECHNOLOGY LETTERS, IEEE INC. NEW YORK, US, vol. 9, no. 8, 1 August 1997 (1997-08-01), pages 1063-1065, XP000699799 ISSN: 1041-1135 figures 1,2	1-8
A	SUN D C ET AL: "HIGH POWER AND HIGH EFFICIENCY VERTICAL CAVITY SURFACE EMITTING GAAS LASER" APPLIED PHYSICS LETTERS, AMERICAN INSTITUTE OF PHYSICS. NEW YORK, US, vol. 61, no. 13, 28 September 1992 (1992-09-28), pages 1502-1503, XP000307067 ISSN: 0003-6951 abstract	1
A	WANG-HUA XIANG ET AL: "FEMTOSECOND EXTERNAL-CAVITY SURFACE-EMITTING INGAAS/INP MULTIPLE-QUANTUM-WELL LASER" OPTICS LETTERS, OPTICAL SOCIETY OF AMERICA, WASHINGTON, US, vol. 16, no. 18, 15 September 1991 (1991-09-15), pages 1394-1396, XP000226943 ISSN: 0146-9592 abstract	1

INTERNATIONAL SEARCH REPORT

PCT/GB 01/05387

Patent document cited in search report		Publication date	Patent family member(s)		Publication date
WO 0010234	A	24-02-2000	US	6327293 B1	04-12-2001
			EP	1105952 A1	13-06-2001
			WO	0010234 A1	24-02-2000
WO 9912235	A	11-03-1999	AU	9472298 A	22-03-1999
			WO	9912235 A1	11-03-1999
			US	6263002 B1	17-07-2001
US 5365539	A	15-11-1994	US	5265116 A	23-11-1993
			US	4860304 A	22-08-1989
			US	4953166 A	28-08-1990
			US	5256164 A	26-10-1993
			AT	110499 T	15-09-1994
			CA	1292797 A1	03-12-1991
			DE	68917610 D1	29-09-1994
			DE	68917610 T2	15-12-1994
			EP	0327310 A2	09-08-1989
			EP	0571051 A1	24-11-1993
			ES	2059716 T3	16-11-1994
			JP	2005490 A	10-01-1990
			JP	2074861 C	25-07-1996
			JP	7112082 B	29-11-1995
			US	5402437 A	28-03-1995
			US	5115445 A	19-05-1992
			AU	637787 B2	10-06-1993
			AU	5199590 A	05-09-1990
			CA	2046637 A1	10-08-1990
			CN	1045200 A	05-09-1990
			EP	0457846 A1	27-11-1991
			JP	4503429 T	18-06-1992
			WO	9009688 A1	23-08-1990